Appendix I
Some Properties of the Maxwell-Boltzman (M-B) Velocity Distribution

This distribution is related to the stationary state of a system with temperature T, provided the interactions between particles are sufficiently numerous. If the thermodynamic system is not in complete equilibrium, the minimum requirement is that collisions between particles of the same type be numerous enough for the Maxwell-Boltzmann distribution (in short a Maxwellian distribution) to be established.

M-B distribution in the absence of external fields

In one dimension, using the electrons as an example, the distribution function is given by the expression (Fig. I.1):

$$f(w) = \left(\frac{m_e}{2\pi k_B T}\right)^{1/2} \exp\left[-\frac{m_e w^2}{2k_B T}\right] , \tag{I.1}$$

where m_e is the electron mass, T their temperature, k_B the Boltzmann constant, and w, the microscopic (individual) electron velocity of thermal origin.

In three dimensions, for the case where the particles have a collective motion with velocity $\boldsymbol{v}$, the microscopic velocity distribution depends on the orientation of $\boldsymbol{w}$ with respect to $\boldsymbol{v}$:

$$f(\boldsymbol{w}) = \left(\frac{m_e}{2\pi k_B T}\right)^{3/2} \exp\left[-\frac{m_e}{2k_B T}(\boldsymbol{w}-\boldsymbol{v})^2\right] , \tag{I.2}$$

where $(\boldsymbol{w}-\boldsymbol{v})^2 \equiv w^2 + v^2 - 2\boldsymbol{w}\cdot\boldsymbol{v}$.

Unless otherwise stated, the normalisation condition used here is:

$$\int_{-\infty}^{\infty} f(\boldsymbol{w})\, \mathrm{d}^3 w = 1 \tag{I.3}$$

with $\mathrm{d}^3 w = \mathrm{d}w_x\, \mathrm{d}w_y\, \mathrm{d}w_z$ in Cartesian coordinates.

M. Moisan, J. Pelletier, *Physics of Collisional Plasmas*,
DOI 10.1007/978-94-007-4558-2,

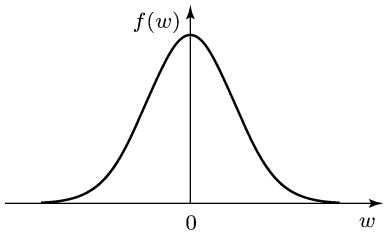

Fig. I.1 Maxwell-Boltzmann distribution in one dimension.

We could also have chosen the normalisation in terms of the electron density:

$$\int_{-\infty}^{\infty} f(\boldsymbol{w})\, \mathrm{d}^3 w = n_e \ . \tag{I.4}$$

In this case, n_e must be included as a factor in (I.2): this is discussed further in Sect. 3.3.

If the group velocity $\boldsymbol{v} = 0$, the distribution is isotropic:

$$f(w) = \left(\frac{m_e}{2\pi k_B T}\right)^{3/2} \exp\left[-\frac{m_e w^2}{2k_B T}\right] \ , \tag{I.5}$$

i.e. it is independent of the direction of the velocity $\boldsymbol{w}$. In this case, the isotropy leads to $\mathrm{d}^3 w = 4\pi w^2\, \mathrm{d}w$ in spherical coordinates, and the distribution of particles, travelling with a scalar (positive) velocity in the interval w, $w + \mathrm{d}w$, is then given by:

$$g(w) \equiv 4\pi w^2 f(w) \tag{I.6}$$

from which:

$$g(w) = \sqrt{\frac{2}{\pi}} \left(\frac{m_e}{k_B T}\right)^{3/2} w^2 \exp\left[-\frac{m_e w^2}{2k_B T}\right] \ , \tag{I.7}$$

which is illustrated in Fig. I.2. The normalisation condition under these conditions is:

$$\int_0^{\infty} g(w)\, \mathrm{d}w = \int_0^{\infty} 4\pi w^2 f(w)\, \mathrm{d}w = 1. \tag{I.8}$$

Characteristic velocities of the M-B distribution with zero group velocity ($\langle \boldsymbol{w} \rangle \equiv \boldsymbol{v} = \mathbf{0}$)

- the *most probable speed*

$$v_{th} = \left(\frac{2k_B T}{m_e}\right)^{1/2} \ , \tag{1.8}$$

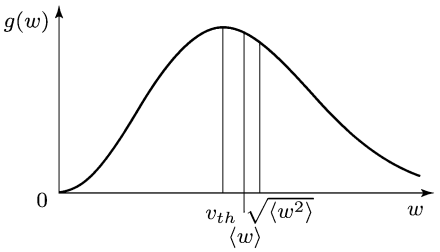

Fig. I.2 Isotropic Maxwell-Boltzmann distribution, represented in scalar form, showing characteristic velocities.

- the *average speed*

$$\langle w \rangle = \left(\frac{8 k_B T}{\pi m_e} \right)^{1/2} = 1.128 \; v_{th} \; , \tag{I.9}$$

- the *mean square speed* (related to the average energy):

$$\sqrt{\langle w^2 \rangle} = \left(\frac{3 k_B T}{m_e} \right)^{1/2} = 1.225 \; v_{th} \; , \tag{I.10}$$

- the *average kinetic energy*

$$\frac{1}{2} m \langle w^2 \rangle = \frac{3}{2} k_B T \; , \tag{I.11}$$

- the *random flux*, defined as the flux of particles traversing a surface in a single direction (in the positive z direction, for example, see exercise 1.2):

$$\langle n w_z \rangle = \frac{n \langle w \rangle}{4} \; . \tag{I.12}$$

M-B distribution in a conservative force field

If a conservative force field $\boldsymbol{F}$ acts on the particles, a prerequisite for a Maxwell-Boltzmann distribution is that this force obeys the relation:

$$\boldsymbol{F} = -\boldsymbol{\nabla} \Phi(\boldsymbol{r}) \tag{I.13}$$

where $\Phi(\boldsymbol{r})$ is the potential energy. The distribution function $f(\boldsymbol{r}, \boldsymbol{w})$ can then be written in the form:

$$f(\boldsymbol{r}, \boldsymbol{w}) = \hat{n}(\boldsymbol{r}) \exp \left[-\frac{\Phi(\boldsymbol{r})}{k_B T} \right] f(\boldsymbol{w}) \tag{I.14}$$

where $\hat{n}(\boldsymbol{r})$ is the density of particles in the absence of applied or space-charge field $\boldsymbol{E}$.

Writing:

$$n(\boldsymbol{r}) = \hat{n}(\boldsymbol{r}) \exp\left[-\frac{\Phi(\boldsymbol{r})}{k_B T}\right] , \tag{I.15}$$

we obtain:

$$f(\boldsymbol{r}, \boldsymbol{w}) = n(\boldsymbol{r}) f(\boldsymbol{w}) , \tag{I.16}$$

which shows that the function $f(\boldsymbol{r}, \boldsymbol{w})$ is separable (Sect. 3.3). Including the normalisation (I.3) for the function $f(\boldsymbol{w})$, this leads to the normalisation condition for $f(\boldsymbol{r}, \boldsymbol{w})$:

$$\int_w f(\boldsymbol{r}, \boldsymbol{w}) \, \mathrm{d}^3 w = n(\boldsymbol{r}) \int_w f(\boldsymbol{w}) \, \mathrm{d}^3 w = n(\boldsymbol{r}) . \tag{I.17}$$

Note that we use the notation f for the velocity distribution function, whether it is separated or not: if the argument of f does not contain the position vector, we can conclude that it has been separated.

Druyvesteyn electron distribution

This distribution is often used in plasma physics, notably because it can be expressed in analytic form. Used conjointly with the M-B distribution function, it allows us to determine the conditions for which certain hydrodynamic parameters depend on the form of the electron energy distribution function (EEDF).

The Druyvesteyn distribution can be considered as an adequate description of the EEDF when the electrons satisfy the four following assumptions [10]:

1. Elastic electron-heavy particle collisions predominate: inelastic collisions (excitation and ionisation) are thus negligible;
2. Electron-electron collisions are negligible;
3. The total microscopic cross-sections for electron-neutral collisions are independent of electron energy for all types of collision;
4. The average electron energy is higher than that of heavy particles ($T_e > T_g$).

For an isotropic distribution, the Druyvesteyn EEDF may be written:

$$f_D(w) = \frac{1.04\pi^{\frac{1}{2}}}{2} \left(\frac{m_e}{2\pi k_B T_e}\right)^{\frac{3}{2}} \exp\left[-0.55 \left(\frac{m_e w^2}{2 k_B T_e}\right)^2\right] . \tag{I.18}$$

Figure I.3 compares the Druyvesteyn distribution with that of Maxwell-Boltzmann's for the same average electron energy and the same electron density: the Druyvesteyn distribution contains much fewer high energy electrons than the M-B distribution.

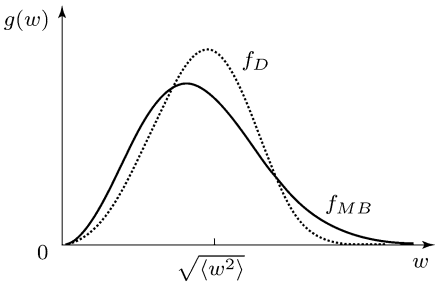

Fig. I.3 Comparison of isotropic Druyvesteyn's and Maxwell-Boltzmann's EEDFs with the same average energy.

M-B electron energy distribution

In Appendix XVII, we show that the Maxwell-Boltzmann distribution function in electron energy U_{eV} can be written:

$$F(U_{eV}) = \frac{2}{\pi^{\frac{1}{2}}(k_B T_e)^{\frac{3}{2}}} \exp\left(-\frac{eU_{eV}}{k_B T_e}\right) , \tag{I.19}$$

where $\bar{U}_{eV} = \frac{3}{2}\frac{k_B T_e}{2e}$ is the average energy.

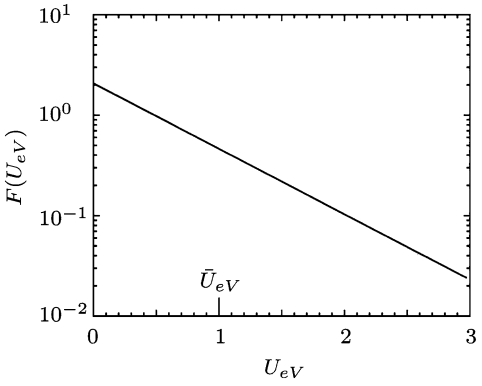

Fig. I.4 Distribution function for Maxwellian electrons of energy U_{eV} with an average energy $\bar{U}_{eV} = 1\,\text{eV}$.

Appendix II
The Complete Saha Equation

The complete Saha equation can be written in the form:

$$\frac{n_{it} n_e}{n_{0t}} = \frac{(2\pi m_e k_B T)^{3/2}}{h^3} \, 2 \, \frac{B'(T)}{B(T)} \, \exp\left[-\frac{e\phi_i}{k_B T}\right] \tag{II.1}$$

where ϕ_i is the first ionisation potential of the neutral atoms, n_{0t} and n_{it} are the *total* density of neutral atoms and the *total* density of ions respectively (total density includes the ground state and all the respective excited states of the neutral atoms and of the ions), n_e is the electron density ($n_e = n_i$ because the ions are only singly ionised); $B(T)$ and $B'(T)$ are the *partition functions* given by:

$$B(T) = \sum_{k=0}^{\infty} g_k \exp\left[-\frac{e\phi_k}{k_B T}\right] \tag{II.2}$$

where the sum over k includes all of the excited states of the atom ($k = 0$ represents the ground state) and:

$$B'(T) = \sum_{j=0}^{\infty} g_j \exp\left[-\frac{e\phi_j}{k_B T}\right] \tag{II.3}$$

where the sum over j includes the excited states of the singly-ionised (positive) ion ($j = 0$ is the ion ground state), g_k and g_j represent the degeneracies of the neutral atom and ion levels, respectively, and ϕ_k and ϕ_j are the potentials (value at threshold, see Sect. 1.7.9) corresponding to the excitation levels (measured with respect to the ground state of the neutral atom or that of the ion, whence $\phi_k(k = 0) = 0$ and $\phi_j(j = 0) = 0$).

M. Moisan, J. Pelletier, *Physics of Collisional Plasmas*,
DOI 10.1007/978-94-007-4558-2,

Significance of the partition function

The density n_m of the excited level m with respect to the density of its ground state (subscript zero) is given by (Boltzmann's law):

$$\frac{n_m}{n_0} = \frac{g_m}{g_0} \exp\left[-\frac{(\mathcal{E}_m - \mathcal{E}_0)}{k_B T}\right] . \tag{1.10}$$

One would like to express n_m as a function of the total density of the neutral atoms n_{0t} (or the ions n_{it}). From the Boltzmann law, the cumulative density n_{0t} becomes:

$$\begin{aligned} n_{0t} \equiv & \sum_{k=0}^{\infty} n_k \\ = & \frac{n_0}{g_0}\left(g_0 + g_1 \exp\left[-\frac{(\mathcal{E}_1 - \mathcal{E}_0)}{k_B T}\right] + \cdots + g_m \exp\left[-\frac{(\mathcal{E}_m - \mathcal{E}_0)}{k_B T}\right] + \cdots\right) . \end{aligned} \tag{II.4}$$

Substituting the definition of the partition function (II.2), the ratio n_m/n_{0t} can be written:

$$\frac{n_m}{n_{0t}} = \frac{g_m}{B(T)} \exp\left[-\frac{(\mathcal{E}_m - \mathcal{E}_0)}{k_B T}\right] . \tag{II.5}$$

Comparing (II.1), the exact form of the Saha law, with its simplified form (1.12), we note that this approximation assumes that $B(T) \simeq g_0$. It actually takes no account of the **excited** neutral atoms in the assessment of the total neutral atom density. This is possible in the case where T is sufficiently low; in this case, the density of the ground state is very large compared to the cumulative density of all the excited atoms.

Appendix III
Partial Local Thermodynamic Equilibrium

When introducing the concept of a two-temperature plasma (Sect. 1.4.3), we have shown that the population of the different energy levels of the neutral atoms are not, in this case, governed by the Boltzmann law (1.10): the neighbouring levels to the ground state have radiative lifetimes sufficiently short compared to the time between electron-neutral collisions, such that they depopulate radiatively rather than by electron-neutral collisions, and therefore fail to satisfy the electron kinetics (Saha's law and Boltzmann's law); on the contrary, the higher levels, those situated beneath the first level of the ionised atom, are in collisional equilibrium with the electrons, and satisfy the Boltzmann law because they experience a much greater number of inelastic collisions than the lower levels[178]; setting $T_{\rm exc} = T_e$, enables us to determine their population concentrations. On the other hand, the gas temperature (principally that of the atoms in the ground state, because they are more numerous), denoted by T_g, is such that $T_g \ll T_e$.

This situation is illustrated in Fig. III.1, where we have reproduced the diagram of the energy levels of the neutral argon atom; to simplify the discussion, these levels have been regrouped according to the orbital electronic configuration to which they belong. In this notation, for the ground state level we have $1s^2\,2s^2\,3s^2\,3p^6$, although in Fig. III.1 we have retained only the last term, for simplicity. The first excited configuration, denoted $4s$, contains 4 levels (see the inset) that will be treated as a block.

To verify the applicability of the Boltzmann law, we can draw the logarithm of the population concentration of the neutral atom levels as a function of their energy, with reference to the ground state (1.10), which is called a Boltzmann curve. If the law is satisfied, a straight line is obtained, proportional to $T_{\rm exc}^{-1}$. Fig. III.2, obtained by optical emission spectroscopy in an argon plasma sustained by a microwave discharge at atmospheric pressure,

[178] The electron energy distribution (Sect. 1.4.2 and Appendix I) contains more low energy electrons than high energy electrons, while the collisional excitation of the first levels of the argon atom from the ground state, for example, requires very high energy electrons (above 11.55 eV).

M. Moisan, J. Pelletier, *Physics of Collisional Plasmas*,
DOI 10.1007/978-94-007-4558-2,

shows that the orbital electronic configurations $5p$ and above are in Boltzmann equilibrium among themselves, while the concentrations of the $4p$ configuration fall below this line: the Boltzmann equilibrium is thus only partial with $T_g \ll T_e$ (Sect. 1.4.3).

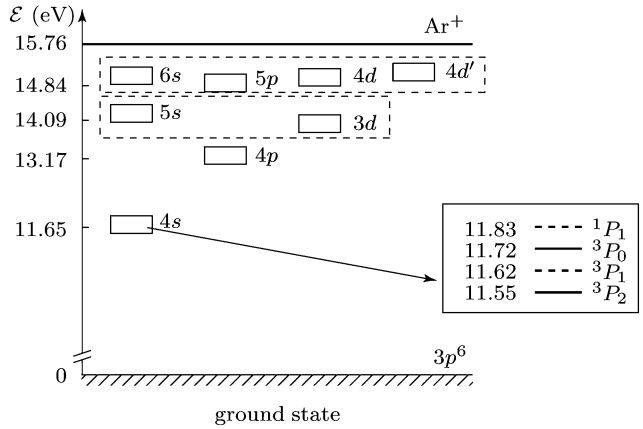

Fig. III.1 Energy diagram of the neutral argon atom, up to the first level of the ionised atom. The energy states have been regrouped according to the orbital electronic configuration to which they belong.

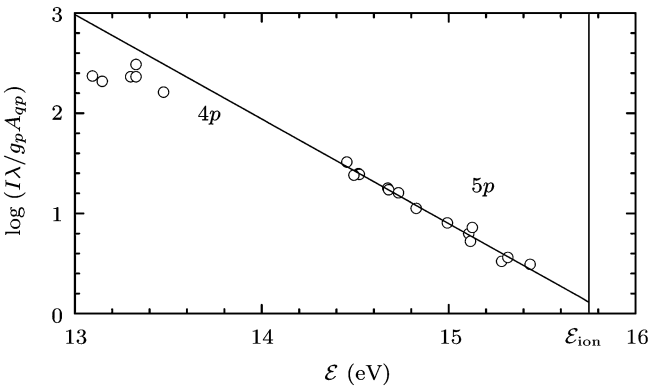

Fig. III.2 Diagram, referred to as a *Boltzmann diagram*, observed in a microwave-discharge in argon (surface wave plasma). The population concentration of the levels is proportional to the intensity I of the radiation emitted at the energy of the levels, expressed in eV, and referenced to the ground state energy; the coefficient A_{qp} represents the frequency of the spontaneous electric-dipolar radiation transition, from the state q to the state p [3].

Appendix IV
Representation of Binary Collisions in the Centre of Mass and Laboratory Frames

In the laboratory frame

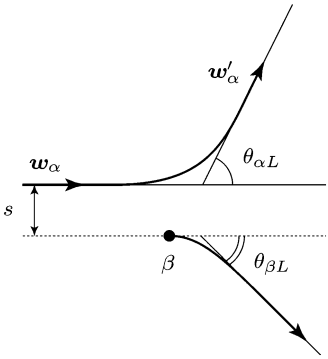

Fig. IV.1 Schematic of a binary collision in the laboratory frame, with impact parameter s: the particle β is assumed to be initially at rest.

In the center of mass frame

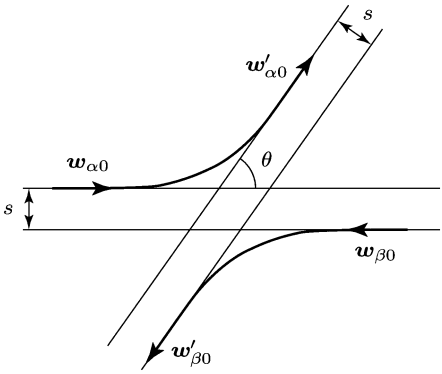

Fig. IV.2 Schematic of a binary collision in the centre of mass frame, showing the scattering angle θ. The distance s between the two pairs of asymptotes is the *impact parameter*.

M. Moisan, J. Pelletier, *Physics of Collisional Plasmas*,
DOI 10.1007/978-94-007-4558-2,

The velocities before and after the collision are parallel and anti-parallel respectively. The representation of the interaction in the centre of mass (CM) frame greatly simplifies the description of the collisional interaction, since a single angle θ completely describes the scattering process.

Relationship between the two frames

From Fig. IV.3, we find:

$$\tan\theta_{\alpha L} = \frac{w'_{\alpha 0}\sin\theta}{w'_{\alpha 0}\cos\theta + w_0} \ . \tag{IV.1}$$

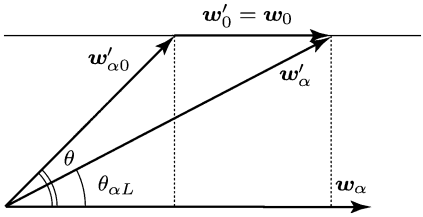

Fig. IV.3 Description, in the most general case, of the velocity of the particle α before and after collision, in the laboratory frame and that of the centre of mass, showing the relationship between the two frames.

The case where particle β is initially at rest:

- If $m_\alpha \ll m_\beta$, the velocity of the CM in the laboratory frame is the same as the velocity of the particle β (1.69). Since it is assumed at rest, then from (1.67) $\boldsymbol{w}_0 \simeq 0$. In this case (IV.1):

$$\theta_{\alpha L} = \theta \ . \tag{IV.2}$$

- If $m_\alpha = m_\beta$ and since $\boldsymbol{w}_\beta = 0$ in the present case, then from (1.72) $\boldsymbol{w}_{\alpha\beta} = \boldsymbol{w}_\alpha$. The velocity of the CM in the laboratory frame is given by (1.69) and can be written:

$$\boldsymbol{w}_0 = \frac{1}{2}\boldsymbol{w}_\alpha = \frac{1}{2}\boldsymbol{w}_{\alpha\beta} \ . \tag{IV.3}$$

Similarly, according to (1.73), the velocity $\boldsymbol{w}_{\alpha 0}$ of the particle α in the CM frame is given by:

$$\boldsymbol{w}_{\alpha 0} = \frac{1}{2}\boldsymbol{w}_{\alpha\beta} \ . \tag{IV.4}$$

Since $w'_{\alpha 0} = w_{\alpha 0}$ in the case of an elastic collision (1.98), (IV.3) and (IV.4) give $w'_{\alpha 0} = w_0$ and finally, from the trigonometric relation (IV.1):

$$\theta_{\alpha L} = \frac{\theta}{2} \ . \tag{IV.5}$$

Appendix V
Limiting the Range of the Coulomb Collisional Interactions: the Coulomb Logarithm

The ultimate objective of this Appendix is to calculate the collision frequencies of the Coulomb interactions, knowing that weak interactions (small scattering angles θ) prevent the corresponding integrals taken over θ from converging (Sect. 1.7.4). These weak interactions have, in fact, no physical importance, when their radius of influence is greater than the Debye length, λ_D: there is electrostatic screening. Accounting for this allows us to reduce the range of integration in θ and thus ensure the convergence of the integrals by introducing the concept of the Coulomb logarithm. To reach this goal, we will first determine the value of θ during a binary elastic collision due to an unspecified central force F.

General study of the trajectories of two particles (binary interactions) subjected to a central force field

Here, we only consider binary, elastic, electromagnetic[179] interactions. This is the case for Van Der Waals interactions between neutrals[180] (potential varies as r^{-6}), between neutral and charged particles[181] (potential varies as r^{-4}) and the Coulomb interactions between charged particles[182] (potential varies as r^{-1}). These electromagnetic interactions induce a conservative central field

[179] The use of the term "electromagnetic interaction" is justified in the two following notes at the foot of this page. On the other hand, the interactions are quantum in nature if the particles approach within a minimum distance that is of the same order of magnitude as the particle dimensions.

[180] Interaction between the instantaneous electric dipole of one of the particles, and the dipole that it induces in the second particle.

[181] Interaction between the charge of one particle, and the electric dipole that it induces in the neutral particle.

[182] We assume that the velocities of the charged particles are sufficiently small, such that the radiation due to the particle deceleration, when deflected by another charged particle (braking radiotion: bremsstrahlung) can be neglected.

M. Moisan, J. Pelletier, *Physics of Collisional Plasmas*,
DOI 10.1007/978-94-007-4558-2,

of force $\boldsymbol{F}$ (see Appendix I), collinear with $\boldsymbol{r}$, such that $\boldsymbol{F} = -\boldsymbol{\nabla}\Phi(r)$ (1.16), where $\Phi(r)$ is the potential energy of the interaction between the particles separated by a distance r.

The geometry of the elastic interaction between two particles α and β is described in Fig. V.1a for a repulsive interaction and in Fig. V.1b for the case of an attractive interaction. In the centre of mass frame (where the centre of gravity G of α and β moves at a constant velocity in the laboratory frame, Sect. 1.7.2), the trajectories of α and β approaching from infinity are two similar curves with respect to G (hyperbola in the particular case of a Coulomb interaction[183]), each having two asymptotes (trajectories a long time before and a long time after the collision). The distance s between the two pairs of asymptotes is the impact parameter (see Fig. V.1). This is also the distance of closest approach in the abscence of interaction.

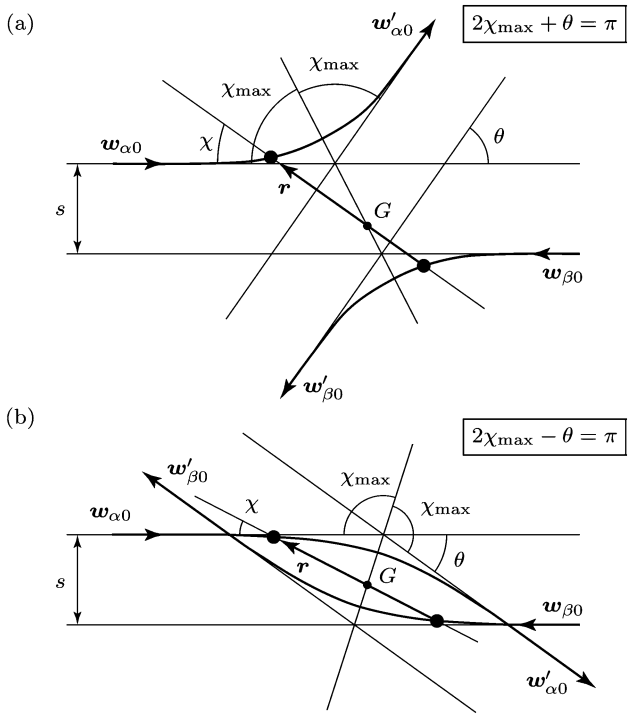

Fig. V.1 Geometric representation of a binary interaction in the barycentric frame (centre of mass): **a** repulsive interaction; **b** attractive interaction. The polar coordinates r and χ describe the position of the particle α with respect to particle β. The value $\chi_{\max}$ corresponds to the minimum value of the distance r.

[183] In the case of $1/r^2$ interaction forces (gravitation and Coulomb forces), the trajectories are either elliptic or hyperbolic.

The study of the motion of the particles is conducted in the centre of mass frame in polar coordinates, with r the distance between the particles α and β (one of the particles taken to be at the origin) and χ the angle between the vector $\boldsymbol{r}$ and the relative velocity $\boldsymbol{w}_{\alpha\beta} = \boldsymbol{w}_{\alpha 0} - \boldsymbol{w}_{\beta 0}$ of the particles α and β before the interaction: the velocities $\boldsymbol{w}_{\alpha 0}$ and $\boldsymbol{w}_{\beta 0}$ of the particles α and β before collision are collinear with $\boldsymbol{w}_{\alpha\beta}$ (1.71) and the velocities $\boldsymbol{w}'_{\alpha 0}$ and $\boldsymbol{w}'_{\beta 0}$ of the particles α and β after collision are collinear with $\boldsymbol{w}'_{\alpha\beta}$. In this system of coordinates, the components of the relative velocity $\boldsymbol{w}$ during the interaction (before the interaction $\boldsymbol{w} = \boldsymbol{w}_{\alpha\beta}$, after the interaction $\boldsymbol{w} = \boldsymbol{w}'_{\alpha\beta}$) are expressed respectively by:

$$w_r = \frac{\mathrm{d}r}{\mathrm{d}t} \,, \quad w_\chi = r\frac{\mathrm{d}\chi}{\mathrm{d}t} \,, \quad w_z = 0 \,, \tag{V.1}$$

where the z axis is perpendicular to the plane (r,χ) containing the trajectories.

In the centre of mass frame, the total kinetic energy related to the sole relative motion of the particles α and β is simply expressed by:

$$\mathcal{E}_c = \frac{\mu_{\alpha\beta} w^2}{2} \,, \tag{1.79}$$

or as a function of the different components of the relative velocity:

$$\mathcal{E}_c = \frac{\mu_{\alpha\beta}}{2}\left[\left(\frac{\mathrm{d}r}{\mathrm{d}t}\right)^2 + r^2\left(\frac{\mathrm{d}\chi}{\mathrm{d}t}\right)^2\right] \,. \tag{V.2}$$

We can easily verify that the kinetic moment of the relative motion, defined by:

$$\boldsymbol{L} = \boldsymbol{r} \wedge \mu_{\alpha\beta}\boldsymbol{w} \tag{V.3}$$

is an invariant of the motion. In fact:

$$\frac{\partial \boldsymbol{L}}{\partial t} = \underbrace{\boldsymbol{w} \wedge \mu_{\alpha\beta}\boldsymbol{w}}_{0} + \boldsymbol{r} \wedge \mu_{\alpha\beta}\frac{\mathrm{d}\boldsymbol{w}}{\mathrm{d}t} \,, \tag{V.4}$$

or again:

$$\frac{\partial \boldsymbol{L}}{\mathrm{d}t} = \boldsymbol{r} \wedge \boldsymbol{F} \equiv 0 \,, \tag{V.5}$$

since $\boldsymbol{r}$ and $\boldsymbol{F}$ are collinear. The calculation of the vector product of the relative kinetic moment $\boldsymbol{L}$ shows that the sole non-zero component is L_z:

$$L_z = \mu_{\alpha\beta} r^2 \frac{\mathrm{d}\chi}{\mathrm{d}t} \tag{V.6}$$

which, from (V.5), is therefore constant during the motion (first invariant of the motion). The value of L_z:

$$L_z = (\boldsymbol{r} \wedge \mu_{\alpha\beta}\boldsymbol{w})_z \tag{V.7}$$

is then easily obtained from the initial conditions at infinity in (V.3), such that:

$$L_z = s\mu_{\alpha\beta} w_{\alpha\beta} = s\mu_{\alpha\beta}(w_{\alpha 0} - w_{\beta 0}) \,, \tag{V.8}$$

where $w_{\alpha\beta}$ is the modulus of the relative velocity $\boldsymbol{w}$ at infinity and, following (V.7), where s, the impact parameter, is the projection of $\boldsymbol{r}$ perpendicularly to $\boldsymbol{w}_{\alpha\beta}$ in the plane containing the trajectories.

A second invariant of the motion is the total energy $\mathcal{E}$ (kinetic energy plus potential energy) which is conserved during the course of the interaction, i.e.:

$$\mathcal{E} = \mathcal{E}_c(r) + \Phi(r) = \text{constant} \,. \tag{V.9}$$

The value of $\mathcal{E}$ is given by the initial conditions before the interaction, when the potential energy is zero, thus:

$$\mathcal{E} = \frac{\mu_{\alpha\beta}}{2} w_{\alpha\beta}^2 \,. \tag{V.10}$$

The equation for the trajectory $\chi = \chi(r)$, which we will now calculate, can be simply deduced from the two invariants. From (V.2) and (V.6), we can write:

$$\mathcal{E} = \frac{\mu_{\alpha\beta}}{2} \left(\frac{\mathrm{d}r}{\mathrm{d}t}\right)^2 + \frac{L_z^2}{2\mu_{\alpha\beta} r^2} + \Phi(r) \,, \tag{V.11}$$

from which:

$$\frac{\mathrm{d}r}{\mathrm{d}t} = \pm\sqrt{\frac{2}{\mu_{\alpha\beta}}\left[\mathcal{E} - \Phi(r)\right] - \left(\frac{L_z}{\mu_{\alpha\beta} r}\right)^2} \,. \tag{V.12}$$

Since:

$$\frac{\mathrm{d}r}{\mathrm{d}t} = \frac{\mathrm{d}r}{\mathrm{d}\chi}\frac{\mathrm{d}\chi}{\mathrm{d}t} \,, \tag{V.13}$$

the differential equation for the trajectory can be directly deduced from (V.6) and (V.12), such that:

$$\frac{\mathrm{d}\chi}{\mathrm{d}r} = \pm\frac{\dfrac{L_z}{\mu_{\alpha\beta} r^2}}{\sqrt{\dfrac{2}{\mu_{\alpha\beta}}\left[\mathcal{E} - \Phi(r)\right] - \left(\dfrac{L_z}{\mu_{\alpha\beta} r}\right)^2}} \tag{V.14}$$

or, by replacing $\mathcal{E}$ and L_z by their values ((V.8) and (V.10)):

$$\frac{\mathrm{d}\chi}{\mathrm{d}r} = \pm\frac{s}{r^2\sqrt{1 - \dfrac{s^2}{r^2} - \dfrac{2\Phi(r)}{\mu_{\alpha\beta} w_{\alpha\beta}^2}}} \,. \tag{V.15}$$

The equation of the trajectory can be obtained by a simple integration over r, provided that the form of the potential energy $\Phi(r)$ of the interaction is known.

The domain of possible values for r is defined by the quantity under the square root, which must remain positive. In particular, the minimum distance $r_{\min}$ between the particles during their interaction is obtained when $\mathrm{d}r/\mathrm{d}\chi = 0$, i.e., when the quantity under the square root in (V.15) is zero:

$$\Phi(r_{\min}) = \frac{\mu_{\alpha\beta} w_{\alpha\beta}^2}{2} \left(1 - \frac{s^2}{r_{\min}^2}\right) . \tag{V.16}$$

The minimum value $r_{\min}$ corresponds to the maximum angle χ, $\chi_{\max}$. In fact, during the motion, while r decreases from infinity to the minimum value $r_{\min}$, the angle χ increases from 0 to $\chi_{\max}$. The angle $\chi_{\max}$ is half the angle between the asymptotes before and after the collision. In the case of a repulsive interaction (Fig. V.1a), the angle $\chi_{\max}$ is linked to θ by the relation:

$$\theta = \pi - 2\chi_{\max} , \tag{V.17}$$

where the scattering angle θ, together with the impact parameter s, is one of the important characteristics of a binary collision. The angle $\chi_{\max}$ is obtained by integration of (V.15) along r from infinity to $r_{\min}$:

$$\chi_{\max} = \int_{\infty}^{r_{\min}} \frac{s \, \mathrm{d}r}{r^2 \sqrt{1 - \left(\frac{s}{r}\right)^2 - \frac{2\Phi(r)}{\mu_{\alpha\beta} w_{\alpha\beta}^2}}} . \tag{V.18}$$

We have now established the general relations describing the trajectories (repulsive and attractive) of the interaction in the case of any central force. To apply these results to specific cases, we need to know the expression for the central force, or $\Phi(r)$, which will allow us to calculate $\chi_{\max}(s, w_{\alpha\beta})$, then finally the scattering angle θ.

Remark: All the preceding calculations have been performed in the centre of mass frame. However, the trajectory in the laboratory frame is almost the same as that calculated in the centre of mass frame if $m_\alpha \ll m_\beta$. In this case, the centre of mass is practically indistinguishable from the case in which the particle β is assumed to be stationary and the scattering angle θ remains unchanged from one frame to the other. On the other hand, if the masses m_α and m_β are similar, the scattering angle approaches $\theta/2$ in the laboratory frame (see Appendix IV).

We will now calculate the angle θ explicitly for the case of a Coulomb interaction.

Scattering angle θ for the specific case of a Coulomb interaction

The electrostatic interaction potential created by the particle β of charge Z_β is:

$$\phi(r) = \frac{1}{4\pi\epsilon_0}\frac{eZ_\beta}{r} \tag{V.19}$$

and the potential energy for the interaction of particle α of charge Z_α with the particle β has the value:

$$\Phi(r) = eZ_\alpha\phi(r)\ , \tag{V.20}$$

hence:

$$\Phi(r) = \frac{Z_\alpha Z_\beta\, e^2}{4\pi\epsilon_0 r}\ . \tag{V.21}$$

We can then define the *critical impact parameter* s_0 (the significance of which will become apparent later) such that:

$$\frac{s_0}{r} = \frac{\Phi(r)}{2\mathcal{E}} \equiv \frac{\Phi(r)}{\mu_{\alpha\beta}w_{\alpha\beta}^2}\ . \tag{V.22}$$

For $Z_\alpha = Z_\beta = 1$, the repulsive case resulting from two positive charges, we have:

$$s_0 = \frac{e^2}{4\pi\epsilon_0\mu_{\alpha\beta}w_{\alpha\beta}^2}\ . \tag{V.23}$$

Substituting (V.22), (V.18) can be written explicitly:

$$\chi_{\max} = \int_\infty^{r_{\min}} \frac{s\,\mathrm{d}r}{r^2\sqrt{1+\left(\frac{s_0}{s}\right)^2 - \left(\frac{s}{r}+\frac{s_0}{s}\right)^2}}\ . \tag{V.24}$$

By a change of variable:

$$\xi = \frac{\frac{s}{r}+\frac{s_0}{s}}{\sqrt{1+\left(\frac{s_0}{s}\right)^2}}\ , \tag{V.25}$$

Eq. (V.24) takes the form:

$$\chi_{\max} = \int_{\xi_\infty}^{1} \frac{-\mathrm{d}\xi}{\sqrt{1-\xi^2}}\ , \tag{V.26}$$

where ξ_∞ is the value of ξ when r tends to infinity, such that:

$$\xi_\infty = \frac{s_0/s}{\sqrt{1+(s_0/s)^2}}\ . \tag{V.27}$$

It should be noted that the upper limit of integration $r_{\min}$ in (V.24) corresponds to $\mathrm{d}r/\mathrm{d}t = 0$, i.e. when the quantity under the square root in (V.12) ia zero, corresponding to $\xi = 1$ in (V.26). The integration of (V.26) thus leads to:

$$\chi_{\max} = \text{arc cos } \frac{s_0/s}{\sqrt{1 + (s_0/s)^2}} , \tag{V.28}$$

hence:

$$\cos \chi_{\max} = \frac{s_0/s}{\sqrt{1 + (s_0/s)^2}} . \tag{V.29}$$

Substituting (V.17), we obtain:

$$\sin(\theta/2) = \cos \chi_{\max} . \tag{V.30}$$

Finally, knowing that:

$$\sin^2(\theta/2) = \frac{1}{1 + \cot^2(\theta/2)} = \frac{(s_0/s)^2}{1 + (s_0/s)^2} , \tag{V.31}$$

we arrive at the formula:

$$\cot(\theta/2) = s/s_0 , \tag{V.32}$$

which gives the expression for the scattering angle θ for a Coulomb collision. This deflection value is a function of the impact parameter s, of s_0 (V.23), of the relative velocity $w_{\alpha\beta}$ of the particles α and β before their interaction. Note that $\theta = \pi/2$ if $s = s_0$, while $\theta = \pi$ if $s = 0$, and the collision is head-on. It follows that if $s < s_0$, the deflection, i.e. the interaction, is important ($\theta > \pi/2$), and weak if $s > s_0$ ($\theta < \pi/2$). We now begin to see the importance of the parameter s_0 for Coulomb interactions.

Total microscopic cross-section for a Coulomb interaction

The differential relation between the total microscopic collision cross-section $\hat{\sigma}_{tc}$ and the microscopic differential scattering cross-section $\hat{\sigma}(\theta)$ can be deduced from (1.110), i.e.:

$$\mathrm{d}\hat{\sigma}_{tc} = 2\pi\hat{\sigma}(\theta) \sin\theta \, \mathrm{d}\theta , \tag{V.33}$$

where $\mathrm{d}\hat{\sigma}_{tc}$ is the *microscopic cross-section element*. From Fig. V.2, this can be expressed as a function of the impact parameter, to give:

$$\mathrm{d}\hat{\sigma}_{tc} = 2\pi s \, \mathrm{d}s . \tag{V.34}$$

In order to make use of $\hat{\sigma}(\theta)$, we can express the microscopic cross-section element $2\pi s\mathrm{d}s$ as a function of the solid angle element $2\pi \sin\theta \mathrm{d}\theta$ from (V.32).

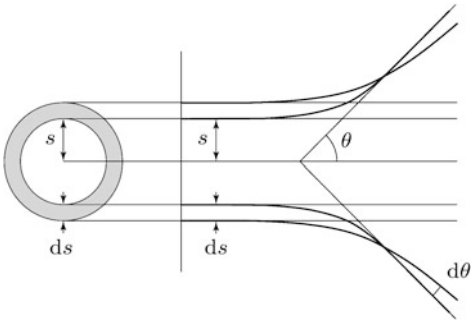

Fig. V.2 Schematic description of the geometric relation between the impact parameter s and the scattering angle θ for a Coulomb binary interaction, where the shaded surface represents the microscopic cross-section element $\mathrm{d}\hat{\sigma}_{tc} = 2\pi s\,\mathrm{d}s$.

After squaring of (V.32), and differentiating, we find:

$$\frac{2s\,\mathrm{d}s}{s_0^2} = -\frac{\left[\cos(\theta/2)\sin^3(\theta/2) + \cos^3(\theta/2)\sin(\theta/2)\right]\,\mathrm{d}\theta}{\sin^4(\theta/2)}\,, \tag{V.35}$$

hence:

$$\frac{2s\,\mathrm{d}s}{s_0^2} = -\frac{1}{2}\,\frac{\sin\theta\,\mathrm{d}\theta}{\sin^4(\theta/2)}\,. \tag{V.36}$$

By comparing (V.36) with (V.33) and (V.34), we deduce that:

$$\hat{\sigma}(\theta) = \left|-\frac{s_0^2}{4\sin^4(\theta/2)}\right|\,. \tag{V.37}$$

The negative sign in (V.37) simply implies that the scattering angle θ decreases as the impact parameter s increases, (V.32), but we shall use the absolute value of the RHS as an expression for the microscopic differential cross-section. Substituting (V.23) into (V.27), for Coulomb collisions, leads to the expression:

$$\hat{\sigma}(\theta,\, w_\infty) = \frac{\left(e^2/8\pi\epsilon_0\mu_{\alpha\beta}w_{\alpha\beta}^2\right)^2}{\sin^4(\theta/2)}\,, \tag{V.38}$$

which allows us, a priori, to calculate the effective total microscopic collision cross-section:

$$\hat{\sigma}_{tc} = \frac{\pi s_0^2}{2}\int_0^\pi \frac{\sin\theta\,\mathrm{d}\theta}{\sin^4(\theta/2)} \tag{V.39}$$

and the momentum transfer cross-section (1.111):

$$\hat{\sigma}_{tm} = \frac{\pi s_0^2}{2}\int_0^\pi \frac{(1-\cos\theta)\sin\theta\,\mathrm{d}\theta}{\sin^4(\theta/2)}\,. \tag{V.40}$$

Unfortunately, it is easy to verify that the integral in (V.39) diverges at $\theta = 0$. This is due to the fact that Coulomb forces are very long range, and in consequence, the distant particles, whose scattering angles approach $\theta = 0$ (un-deviated particles) all contribute to this integral, hence its divergence. The same is true for the integral in (V.40) which, as will be shown in the following calculation, also diverges for $\theta = 0$.

Total microscopic momentum cross-section for Coulomb's interactions

Concept of the Coulomb logarithm

The total cross-section for transfer of momentum (V.40) can also be written as a function of $\theta/2$, in the form:

$$\hat{\sigma}_{tm} = 4\pi s_0^2 \int_0^{\pi} \frac{\mathrm{d}\big[\sin(\theta/2)\big]}{\sin(\theta/2)} \,, \tag{V.41}$$

such that, after integration:

$$\hat{\sigma}_{tm} = 4\pi s_0^2 \, \ln\big[\sin(\theta/2)\big]\Big|_0^{\pi} \,. \tag{V.42}$$

We can verify that, as in the case of $\hat{\sigma}_{tc}$, the cross-section $\hat{\sigma}_{tm}$ diverges since the innumerable long-range collisions for which $\theta \simeq 0$, are taken into account. However, in a plasma, the range of the electric field created by a charged particle is reduced by the screening effect of the neighbouring charged particles and is, in fact, limited by the Debye sphere (Sect. 1.6). Consequently, any two charged particles in a plasma, separated by a distance $r > \lambda_D$, neither "sees" the field of the other particle, and therefore should not be included in the Coulomb interaction. The integration must therefore be limited to particles having an impact parameter s that is smaller than the Debye length ($s < \lambda_D$), i.e. to scattering angles θ greater than the minimum value $\theta_{\min}$ ($\theta < \theta_{\min}$) defined by:

$$\cot\frac{\theta_{\min}}{2} = \frac{\lambda_D}{s_0} \,, \tag{V.43}$$

that is, since $\theta_{\min}$ is small:

$$\frac{\theta_{\min}}{2} \simeq \frac{s_0}{\lambda_D} \,. \tag{V.44}$$

Applying this new limit of integration to (V.42), and setting:

$$\Lambda_c \equiv \frac{\lambda_D}{s_0} \,, \tag{V.45}$$

we obtain the well known expression for the total microscopic momentum transfer cross-section:

$$\hat{\sigma}_{tm} = 4\pi s_0^2 \ln \Lambda_c \ , \tag{V.46}$$

where the parameter $\ln \Lambda_c$ is referred to as the *Coulomb logarithm*.

Remark: Using the same integration limits as for $\hat{\sigma}_{tm}$, the total microscopic collision cross-section can be written:

$$\hat{\sigma}_{tc} = \pi \lambda_D^2 \ . \tag{V.47}$$

This result reflects the fact that **all** Coulomb interactions should be taken into account, provided they are within the Debye sphere ($s \leq \lambda_D$).

Coulomb logarithms for particles satisfying a Maxwellian distribution

The expression for the total microscopic momentum transfer cross-section in (V.46) requires the values of λ_D and s_0, which can be obtained by assuming that the population of charged particles α and β satisfy Maxwellian distributions, with temperatures T_α and T_β.

The Debye length λ_D is, in principle, the global Debye length defined by (1.41). In fact, following Delcroix (1959), the duration of a collision is too short for the screening action of the ions to have an effect, and it is preferable to use $\lambda_D = \lambda_{De}$, the electronic Debye length, in the expression for Λ_c, i.e.:

$$\lambda_{De} = \left(\frac{\epsilon_0 k_B T_e}{n e^2} \right)^{\frac{1}{2}} \ . \tag{1.41}$$

This expression is also consistent with the assumption that the ions constitute a neutralizing background for the electrons (see remark 8, Sect. 1.6).

For the critical impact parameter s_0, we need to calculate $\langle s_0 \rangle$, its mean averaged value $\mu_{\alpha\beta} w_{\alpha\beta}^2$, i.e.:

$$\langle \mu_{\alpha\beta} w_{\alpha\beta}^2 \rangle = \mu_{\alpha\beta} \langle (\boldsymbol{w}_{\alpha 0} - \boldsymbol{w}_{\beta 0})^2 \rangle \ , \tag{V.48}$$

knowing that:

$$\boldsymbol{w}_{\alpha 0} - \boldsymbol{w}_{\beta 0} = \boldsymbol{w}_{\alpha\beta} \ . \tag{1.69}$$

It follows that:

$$\langle \mu_{\alpha\beta} w_{\alpha\beta}^2 \rangle = \mu_{\alpha\beta} \langle w_{\alpha 0}^2 + w_{\beta 0}^2 - 2 \boldsymbol{w}_{\alpha 0} \cdot \boldsymbol{w}_{\beta 0} \rangle \ , \tag{V.49}$$

where the average of $\boldsymbol{w}_{\alpha 0} \cdot \boldsymbol{w}_{\beta 0}$ is zero since all the initial relative directions of the particles in the laboratory frame are equally probable. For Maxwellian distributions, we find, following (I.11):

$$\langle \mu_{\alpha\beta} w_{\alpha\beta}^2 \rangle = \frac{m_\alpha m_\beta}{m_\alpha + m_\beta} \left(\frac{3 k_B T_\alpha}{m_\alpha} + \frac{3 k_B T_\beta}{m_\beta} \right) \ . \tag{V.50}$$

If $T_e = T_i = T$, $\langle s_0 \rangle$ takes a unique value, independent of the nature of the collisions, electron-electron, ion-ion or ion-electron:

$$\langle s_0 \rangle = \frac{e^2}{12\pi\epsilon_0 k_B T} \, . \tag{V.51}$$

On the other hand, if $T_e \neq T_i$, we can distinguish three mean critical impact parameters:

- for electron-electron collisions:

$$s_{0_{ee}} = \frac{e^2}{12\pi\epsilon_0 k_B T_e} \, , \tag{V.52}$$

- for ion-ion collisions:

$$s_{0_{ii}} = \frac{e^2}{12\pi\epsilon_0 k_B T_i} \, , \tag{V.53}$$

- and, for ion-electron collisions:

$$s_{0_{ei}} = s_{0_{ie}} = \frac{e^2 \left(\dfrac{1}{m_e} + \dfrac{1}{m_i} \right)}{12\pi\epsilon_0 \left(\dfrac{k_B T_e}{m_e} + \dfrac{k_B T_i}{m_i} \right)} \, . \tag{V.54}$$

There are three corresponding Coulomb logarithms, $\ln \Lambda_{c_{ee}}$, $\ln \Lambda_{c_{ii}}$ and $\ln \Lambda_{c_{ei}}$. These can be written as functions of $\Lambda_{c_{ee}}$, from the expressions for $s_{0_{\alpha\beta}}$ ($m_e \ll m_i$):

$$\ln \Lambda_{c_{ii}} = \ln \Lambda_{c_{ee}} + \ln \frac{T_i}{T_e} \, , \tag{V.55}$$

and since:

$$s_{0_{ei}} \simeq s_{0_{ee}} \, , \tag{V.56}$$

then:

$$\ln \Lambda_{c_{ei}} \simeq \ln \Lambda_{c_{ee}} \, . \tag{V.57}$$

Coulomb collision frequencies and mean free paths

Collision frequencies for particles satisfying a Maxwellian distribution

Rigorously speaking, the average collision frequency of the species α with the (target) species β is defined by (1.140):

$$\langle \nu_{\alpha\beta}(w_{\alpha\beta}) \rangle = n_\beta \langle \hat{\sigma}_{\alpha\beta}(w_{\alpha\beta}) w_{\alpha\beta} \rangle \tag{V.58}$$

where $\hat{\sigma}_{\alpha\beta}$ is the total microscopic momentum transfer cross-section. However, in the present case of Coulomb collisions, the cross sections calculated

above are already the result of an average taken over the relative velocities, and thus cannot be used to determine the exact expression for (V.58). To do this, it would be necessary to integrate (V.58) over the ensemble of velocities of the populations α and β (in the same way as in exercise 1.9), which leads to a very complex calculation. On the other hand, the collision frequency can be obtained, within an order of magnitude, from the approximate expression:

$$\langle \hat{\sigma}_{\alpha\beta} w_{\alpha\beta} \rangle \simeq \langle \hat{\sigma}_{\alpha\beta} \rangle \langle w_{\alpha\beta} \rangle \ , \tag{V.59}$$

where $\langle w_{\alpha\beta} \rangle$ is the mean velocity.

In fact, it is preferable to define what is called the *individual average collision frequency*, which corresponds to the *most probable relative velocity* $v_{\alpha\beta}$ (distinct from the mean relative velocity). The expression for $v_{\alpha\beta}$ is given by (exercise 1.9):

$$v_{\alpha\beta} = \sqrt{2k_B \left(\frac{T_\alpha}{m_\alpha} + \frac{T_\beta}{m_\beta} \right)} \ . \tag{V.60}$$

The collision frequency is then written:

$$\nu_{\alpha\beta}(v_{\alpha\beta}) = n_\beta \hat{\sigma}_{\alpha\beta}(v_{\alpha\beta})\, v_{\alpha\beta} \ , \tag{V.61}$$

where $\hat{\sigma}_{\alpha\beta}$ is calculated from (V.46), substituting $v_{\alpha\beta}$ for $w_{\alpha\beta}$ in s_0 (V.23):

$$s_{0_{\alpha\beta}} = \frac{e^2}{4\pi\epsilon_0 \mu_{\alpha\beta} v_{\alpha\beta}^2} \ . \tag{V.62}$$

Assuming $T_e \gg T_i$, the collision frequencies can then be written:

$$\nu_{ee} = 4\pi n s_{0_{ee}}^2 \sqrt{\frac{4k_B T_e}{m_e}}\ \ln\left(\frac{\lambda_{De}}{s_{0_{ee}}} \right) \ , \tag{V.63}$$

$$\nu_{ei} = \nu_{ie} \simeq 4\pi n s_{0_{ee}}^2 \sqrt{\frac{2k_B T_e}{m_e}}\ \ln\left(\frac{\lambda_{De}}{s_{0_{ee}}} \right) \ , \tag{V.64}$$

$$\nu_{ii} = 4\pi n s_{0_{ii}}^2 \sqrt{\frac{4k_B T_i}{m_i}}\ \ln\left(\frac{\lambda_{De}}{s_{0_{ii}}} \right) \ . \tag{V.65}$$

It is possible to extract a number of simple relations from (V.63), (V.64) and (V.65). Thus, a first obvious relation:

$$\nu_{ee} \simeq \sqrt{2}\, \nu_{ei} \tag{V.66}$$

shows that the electron-electron and electron-ion collision frequencies are of the same order of magnitude. The second relation, obtained from (V.63):

$$\nu_{ee} = \omega_{pe} \frac{\ln \Lambda_{c_{ee}}}{\Lambda_{c_{ee}}} \tag{V.67}$$

allows us to relate the electron-electron collision frequency to the plasma electron angular frequency ω_{pe}.

Mean free paths for particles satisfying a Maxwellian distribution

Generally speaking, the mean free path of a particle α colliding with particles β can be defined by (1.39):

$$\ell_{\alpha\beta} = \frac{1}{n_\beta} \left\langle \frac{w_\alpha}{\hat{\sigma}_{\alpha\beta}(w_{\alpha\beta}) w_{\alpha\beta}} \right\rangle . \tag{V.68}$$

We define the *average mean free path* for Coulomb collisions, for *the most probable velocities*, in the same way as previously used for the collision frequency, i.e:

$$\ell_{\alpha\beta}(v_\alpha) = \frac{v_\alpha}{n_\beta \hat{\sigma}_{\alpha\beta} v_{\alpha\beta}} . \tag{V.69}$$

The different mean free paths can then be written ($T_e \gg T_i$):

$$\ell_{ee} = \frac{\sqrt{\dfrac{2k_B T_e}{m_e}}}{\nu_{ee}} , \tag{V.70}$$

$$\ell_{ei} = \frac{\sqrt{\dfrac{2k_B T_e}{m_e}}}{\nu_{ei}} , \tag{V.71}$$

$$\ell_{ie} = \frac{\sqrt{\dfrac{2k_B T_i}{m_i}}}{\nu_{ei}} , \tag{V.72}$$

$$\ell_{ii} = \frac{\sqrt{\dfrac{2k_B T_i}{m_i}}}{\nu_{ii}} . \tag{V.73}$$

The mean free path for electrons colliding with all charged particles (electrons and ions) can be written:

$$\ell_e = \frac{\sqrt{\dfrac{2k_B T_e}{m_e}}}{\nu_{ee} + \nu_{ei}} . \tag{V.74}$$

Remark: It is important to note that the Coulomb collision frequencies and the corresponding average mean free paths are independent of the density of the gas.

Appendix VI
Stepwise Ionisation

Two-step, and more generally, multi-step ionisation constitute mechanisms for creating charged particles, which become important whenever the gas pressure exceeds a few torr (a few hundred pascal). Such stepwise processes increase with increasing pressure and electron density to such an extent that they can supersede direct ionisation.

Stepwise ionisation starts with the excitation by an electron collision with the atom in its ground state:

$$\underline{\underline{\mathrm{e}}} + \mathrm{A} \rightarrow \mathrm{A}(j) + \underline{\mathrm{e}} \; . \tag{VI.1}$$

A second electron collision with this atom, which is now excited in the state j, can ionise the atom:

$$\underline{\underline{\mathrm{e}}} + \mathrm{A}(j) \rightarrow \mathrm{A}^{+} + \underline{\mathrm{e}} + \mathrm{e} \; . \tag{VI.2}$$

The excited atom thus serves as an intermediate stage, allowing ionisation with electrons of lower energy than that required for direct ionisation.

Population balance of intermediate (relay) state(s)

The ionisation frequency from the excited state is, by definition:

$$\nu_{ie} = \mathcal{N}_j \langle \hat{\sigma}_{ji}(w) w \rangle \; , \tag{VI.3}$$

where $\mathcal{N}_j$ is the density of atoms in the excited state (the targets for the electrons), $\hat{\sigma}_{ji}$ is the total microscopic cross-section for ionisation from the excited state j, and the square brackets refer to an integration conducted over the velocity distribution function of the particles. To calculate the stepwise ionisation frequency, one needs the density of the atoms excited in state j, which can be determined from the balance of the processes of creation and

M. Moisan, J. Pelletier, *Physics of Collisional Plasmas*,
DOI 10.1007/978-94-007-4558-2,

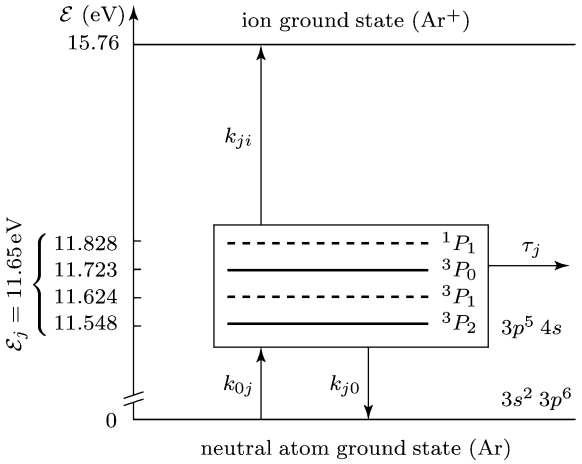

Fig. VI.1 Three-level energy diagram of the argon atom to characterise, in the present case, the two-step ionisation process: these levels are the ground state of the neutral atom, the intermediate state j (the 4 energy states $3p^5\ 4s$ orbital configuration are effectively considered as a single level) and the first level of the ionised atom. The $^3P_0$ and $^3P_2$ levels are metastable states, i.e. they have a comparatively lower probability of de-exciting through a (dipolar electric) radiative transition than the $^1P_1$ and $^3P_1$ levels, which are termed resonance radiation states (also referred to as quasi-metastable states).

loss of atoms in the intermediate state j. This can be established with the help of the three-level energy diagram shown in Fig. VI.1.

In the stationary state, the balance of creation and loss obviously requires that:

$$\frac{\mathrm{d}\mathcal{N}_j}{\mathrm{d}t} = 0\ , \tag{VI.4}$$

where $\mathrm{d}\mathcal{N}_j/\mathrm{d}t$, in the present case, can be written in the following form:

$$\begin{aligned}\frac{\mathrm{d}\mathcal{N}_j}{\mathrm{d}t} &= \mathcal{N}_0\langle\hat{\sigma}_{0j}(w)w\rangle n_e - \mathcal{N}_j\langle\hat{\sigma}_{j0}(w)w\rangle n_e \\ &\quad - \mathcal{N}_j\langle\hat{\sigma}_{ji}(w)w\rangle n_e - \frac{D_j}{\Lambda^2}\mathcal{N}_j\ .\end{aligned} \tag{VI.5}$$

The first term on the RHS represents the way the intermediate state is populated by electron collisions on the atom in the ground state (reaction (VI.1)). The other terms correspond to the depopulation of the intermediate states, successively, as a result of their de-excitation by electron collision to the ground state (the inverse process to reaction (VI.1), by ionisation described by (VI.2), and by diffusion of the atoms to the walls. In equation (VI.5), N_0 is the density of the atoms in the ground state; $k_{0j} \equiv \langle\hat{\sigma}_{0j}(w)w\rangle$ is the electron excitation coefficient from ground state to the state j; $k_{j0} \equiv \langle\hat{\sigma}_{j0}(w)w\rangle$ is the electron de-excitation coefficient from the state j to the ground state and $k_{ji} \equiv \langle\hat{\sigma}_{ji}(w)w\rangle$ is the ionisation coefficient from the excited state j. D_j

is the diffusion coefficient for excited atoms in the plasma and Λ is the characteristic diffusion length ($\Lambda = R/2.405$ in cylindrical geometry, where R is the tube radius; this is described in more detail in Sect. 3.8). The processes included in (VI.5) are represented in Fig. VI.1, where the notation j defines the intermediate state. The diffusion of the atoms in the intermediate stage is represented in the same diagram by their characteristic diffusion time τ_j where (Sect. 3.8):

$$\frac{D_j}{\Lambda^2} = \frac{1}{\tau_j} \,. \tag{VI.6}$$

Two-step ionisation generally occurs from atoms in metastable states as the intermediate stage, because their radiative de-excitation time is very long, such that the depopulation is governed by electron collisions and by diffusion. We obtain the density of the intermediate states in a stationary plasma from equation (VI.5):

$$\mathcal{N}_j = \frac{\mathcal{N}_0 \langle \hat{\sigma}_{0j}(w) w \rangle n_e}{\tau_j^{-1} + \left(\langle \hat{\sigma}_{j0}(w) w \rangle + \langle \hat{\sigma}_{ji}(w) w \rangle \right) n_e} \,. \tag{VI.7}$$

The rate of depopulation of the intermediate stages by diffusion is principally determined by the gas pressure: as gas density increases, the diffusion time τ_j for these atoms also increases, reducing the loss by this mechanism (the two metastable states in Fig. VI.1 are considered as forming one single intermediate stage). When the depopulation of these states by diffusion is much smaller than that due to collisions (i.e. $\tau_j^{-1} \ll \left(\langle \hat{\sigma}_{j0}(w) w \rangle + \langle \hat{\sigma}_{ji}(w) w \rangle \right) n_e$), Eq. (VI.7) shows that the value of $\mathcal{N}_j$ is independent of the electron density: this effect also manifests itself when the electron density is extremely high.

Ionisation frequency

Equation (VI.3), defining the two-step ionisation frequency, with the substitution of $\mathcal{N}_j$ from (VI.7), leads to:

$$\nu_{ie} = \frac{\mathcal{N}_0 \langle \hat{\sigma}_{0j}(w) w \rangle \langle \hat{\sigma}_{ji}(w) w \rangle \tau_j n_e}{1 + \left(\langle \hat{\sigma}_{j0}(w) w \rangle + \langle \hat{\sigma}_{ji}(w) w \rangle \right) \tau_j n_e} \,. \tag{VI.8}$$

Setting:

$$\rho_{ie} = \mathcal{N}_0 \langle \hat{\sigma}_{0j}(w) w \rangle \langle \hat{\sigma}_{ji}(w) w \rangle \tau_j \,, \qquad \text{units: cm}^3\,\text{s}^{-1} \tag{VI.9}$$

which we call the *two-step ionisation coefficient*, and:

$$\eta = \left(\langle \hat{\sigma}_{j0}(w) w \rangle + \langle \hat{\sigma}_{ji}(w) w \rangle \right) \tau_j \,, \qquad \text{units: cm}^3 \tag{VI.10}$$

which we refer to as the *saturation coefficient of intermediate states*. The two-step ionisation frequency can then be written in the form (1.159):

$$\nu_{ie} = \frac{\rho_{ie} n_e}{1 + \eta n_e} \ . \tag{VI.11}$$

The case where the value of ν_{ie} remains constant when n_e increases is referred to as *saturation*; two-step ionisation then clearly exceeds direct ionisation. This situation occurs when the diffusion time τ_j is very large (large value of η) or when the value of n_e is very large. In these conditions, Eq. (VI.11) no longer depends on n_e, since:

$$\nu_{ie} \simeq \frac{\rho_{ie}}{\eta} \ . \tag{1.160}$$

Appendix VII
Basic Notions of Tensors

A tensor is characterised by the transformation required to express it in another frame.

- A scalar s is an invariant quantity with respect to a change of frame. It is a tensor of rank (or order) zero.
- A vector $\boldsymbol{w}$ can be written as:

$$\boldsymbol{w} = w_x \hat{\mathbf{e}}_x + w_y \hat{\mathbf{e}}_y + w_z \hat{\mathbf{e}}_z \ , \tag{VII.1}$$

where $\hat{\mathbf{e}}_x$, $\hat{\mathbf{e}}_y$ and $\hat{\mathbf{e}}_z$ are the basis vectors in a given frame, which we will refer to as the old frame. Following a change of frame, the components $(w_x,\ w_y,\ w_z)$ of $\boldsymbol{w}$ are related to the components in a new frame by a transformation matrix A with elements α^i_j. Writing W^I for the components of $\boldsymbol{w}$ in the new coordinate system, we then have[184]:

$$W^I = \alpha^I_1 w_1 + \alpha^I_2 w_2 + \alpha^I_3 w_3 = \alpha^I_i w^i \tag{VII.2}$$

where, in order to apply the *Einstein summation convention* (to avoid using the summation sign), we have written the indices for the components of $\boldsymbol{w}$ on the RHS of the equation as superscripts. This rule is such that the same index, repeated as subscript and superscript, implies a summation over all its values: the *index* is said to be *dummy* because its name can be arbitrarily changed. Following this notation, the vector $\boldsymbol{w}$ can be represented in compact fashion by $\boldsymbol{w} = w^i \hat{\mathbf{e}}_i$.
The inverse transformation (from the new frame into the old) is made using the matrix B with elements β^i_j, which is the inverse of matrix A of elements (α^i_j); this implies that $(A)(B) = (I)$, where (I) is the identity matrix. Hence, the components of $\boldsymbol{w}$ in the old coordinate system can be written:

[184] If we designate the basis vectors in the new frame by $\hat{\boldsymbol{E}}_x$, $\hat{\boldsymbol{E}}_y$, $\hat{\boldsymbol{E}}_z$, these can be obtained from the basis vectors in the old frame through the relation $\hat{\boldsymbol{E}}_I = \alpha^k_I \hat{\mathbf{e}}_k$.

M. Moisan, J. Pelletier, *Physics of Collisional Plasmas*,
DOI 10.1007/978-94-007-4558-2,

$$w^i = \beta_I^i W^I \ . \tag{VII.3}$$

The vector $\boldsymbol{w}$ is a first-rank tensor.

- A second-rank tensor $\underline{\boldsymbol{T}}$ can be expressed in a given frame as:

$$\underline{\boldsymbol{T}} = t_{xx}\hat{\mathbf{e}}_x\hat{\mathbf{e}}_x + t_{xy}\hat{\mathbf{e}}_x\hat{\mathbf{e}}_y + t_{xz}\hat{\mathbf{e}}_x\hat{\mathbf{e}}_z + \cdots \ , \tag{VII.4}$$

i.e. it requires two basis vectors for each component (written as such, $\underline{\boldsymbol{T}}$ is also termed a dyadic tensor): there are 9 components in total. In consequence, during a change of frame, it is necessary to use the transformation matrix twice. Thus the components of $\underline{\boldsymbol{T}}$ in the new frame are given by:

$$T^{IJ} = \alpha_i^I \alpha_j^J t^{ij} \ . \tag{VII.5}$$

We can generalise the definition of $\underline{\boldsymbol{T}}$ to any particular rank by noting that the number of indices in a tensor, i.e. the number of transformation matrices required during a change of frame, defines the *rank of the tensor.*

Tensor products

- The *tensor product* of two vectors $\boldsymbol{A}$ and $\boldsymbol{B}$, written as $\boldsymbol{A} \otimes \boldsymbol{B}$, is defined by its elements:

$$T_{ij} = A_i B_j \ , \tag{VII.6}$$

where the indices i and j can take the values 1, 2 or 3. This creates a second-rank tensor. The tensor product can be generally applied to a product of two tensors of any order: the rank of the resulting tensor is the sum of the ranks of the tensors which form the product.

- The *scalar product* or internal product is, in tensor formalism, a *contraction*, reducing the order of the initial tensors by two units[185]. Thus, for two vectors $\boldsymbol{A}$ and $\boldsymbol{B}$, this gives (using the implicit summation rule):

$$\boldsymbol{A} \cdot \boldsymbol{B} = \left(A^i \hat{\mathbf{e}}_i\right) \cdot \left(B^j \hat{\mathbf{e}}_j\right) = A^i B^j \hat{\mathbf{e}}_i \cdot \hat{\mathbf{e}}_j = A^i B^j \delta_{ij} = \sum_i A^i B^i \tag{VII.7}$$

where δ_{ij} is the Kronecker delta ($\delta_{ij} = 1$ if $i = j$ and $\delta_{ij} = 0$ if $i \neq j$). To continue to use the implicit summation rule, we must write (VII.7) in the form:

$$\boldsymbol{A} \cdot \boldsymbol{B} = A^i B_i \ . \tag{VII.8}$$

The result is a scalar, i.e. a zero order tensor.

- The *vector product* of two vectors $\boldsymbol{A}$ and $\boldsymbol{B}$ is considered as a vector, but in fact it is a pseudovector. When we move from a right-handed triad to

[185] The scalar product of two vectors can be seen as a tensor product followed by a contraction.

a left-handed one, the pseudovector changes its direction in space, which is contrary to the notion of a true vector (also called a polar vector). In reality, the vector product should be represented by an antisymmetric, second-order tensor, i.e $T_{ij} = -T_{ji}$, which implies that the diagonal elements on the matrix $\underline{\boldsymbol{T}}$ should be zero. This tensor comprises only three independent elements, allowing the vector product to be represented by a vector in 3-dimension space.

Operators

- The *gradient* is an operator that produces a tensor one order higher than that on which it operates. Thus, starting with a scalar s:

$$\boldsymbol{\nabla} s = \frac{\partial s}{\partial x}\hat{\mathbf{e}}_x + \frac{\partial s}{\partial y}\hat{\mathbf{e}}_y + \frac{\partial s}{\partial z}\hat{\mathbf{e}}_z = \sum_i \partial_i s \ \hat{\mathbf{e}}_i \ , \tag{VII.9}$$

  we obtain a vector.
  The convention of dummy indices cannot be applied here, since the operator "spatial derivative" is, strictly speaking, covariant[186] (yielding a subscript index), hence the necessity of writing explicitly the summation sign.
- The *divergence* is the result of the action of a gradient operator followed by a contraction. Thus, the divergence of a vector $\boldsymbol{w}$, $\boldsymbol{\nabla} \cdot \boldsymbol{w}$, is a scalar (see note 74, p. 138): the result is a tensor of one rank lower than the one that is operated on.
- The *curl* acts on a covariant vector with components a_i and produces a covariant, antisymmetric, second-rank tensor with elements b_{ij}:

$$b_{ij} = \frac{\partial a_j}{\partial x^i} - \frac{\partial a_i}{\partial x^j} \ . \tag{VII.10}$$

  This creates a tensor of one order higher than the initial tensor, due to the action of the spatial operator $\partial/\partial x^i$.

Example of the proof of a tensor identity

We wish to show that:

$$\boldsymbol{\nabla}_r \cdot (\boldsymbol{w}\boldsymbol{w} f) = \boldsymbol{w}(\boldsymbol{w} \cdot \boldsymbol{\nabla}_r f) \ . \tag{VII.11}$$

Developing the LHS:

[186] The concept of a covariant derivative is beyond the scope of the present plasma treatise.

$$\boldsymbol{\nabla}_r \cdot \boldsymbol{w}\boldsymbol{w} f = \sum_i \partial_i \left(\hat{\mathbf{e}}_i \cdot \left(w^p w^q \hat{\mathbf{e}}_p \hat{\mathbf{e}}_q \right) f \right) \ , \tag{VII.12}$$

where f is a scalar and ∂_i a derivative operator in position space (which therefore does not act on the microscopic velocities). Note that there is no implicit summation over index i because the two elements carrying this index are covariant. Expanding the product $\hat{\mathbf{e}}_i \cdot \hat{\mathbf{e}}_p = \delta_{ip}$ in (VII.12), which imposes $i = p$ (VII.7), we have:

$$\partial_i \left(\hat{\mathbf{e}}_i \cdot \left(w^p w^q \hat{\mathbf{e}}_p \hat{\mathbf{e}}_q \right) f \right) = \partial_i \left(w^i w^q \hat{\mathbf{e}}_q f \right) = \partial_i \left(f w^i \right) w^q \hat{\mathbf{e}}_q \ , \tag{VII.13}$$

where there is a summation (contraction) over the index i, such that:

$$\partial_i \left(f w^i \right) \boldsymbol{w} = \left(\boldsymbol{\nabla}_r f \cdot \boldsymbol{w} \right) \boldsymbol{w} \ . \tag{VII.14}$$

Finally, because $\boldsymbol{\nabla}_r f \cdot \boldsymbol{w}$ is a scalar, we can write:

$$\left(\boldsymbol{\nabla}_r f \cdot \boldsymbol{w} \right) \boldsymbol{w} = \boldsymbol{w} (\boldsymbol{\nabla}_r f \cdot \boldsymbol{w}) \ , \tag{VII.15}$$

which is the RHS of (VII.11), as required: QED.

Appendix VIII
Operations on Tensors

The fundamental properties of tensors were presented in Appendix VII. We will now give the rules for tensor operations, without recourse to the implicit summation (dummy indices) defined in Appendix VII.

Product of two vectors

Consider two vectors $\boldsymbol{A}$ and $\boldsymbol{B}$, with components A_i and B_i, with $i = x, y, z$ or $i = 1, 2, 3$.

Scalar product of two vectors: $\boldsymbol{A} \cdot \boldsymbol{B}$

The result is a scalar C:

$$\boldsymbol{A} \cdot \boldsymbol{B} = \sum_{i=1}^{3} A_i B_i = \boldsymbol{B} \cdot \boldsymbol{A} = C \,. \tag{VIII.1}$$

The scalar product of two vectors is commutative.

Vector product of two vectors: $\boldsymbol{A} \wedge \boldsymbol{B}$

The result is a vector $\boldsymbol{C}$ (in reality, a pseudovector, Appendix VII) with components:

$$C_i = A_{i+1} B_{i-1} - A_{i-1} B_{i+1} \tag{VIII.2}$$

where, if $i = x$, then $x + 1 = y$ and $x - 1 = z$. It follows that:

$$\boldsymbol{A} \wedge \boldsymbol{B} = -\boldsymbol{B} \wedge \boldsymbol{A} = \boldsymbol{C} \,, \tag{VIII.3}$$

M. Moisan, J. Pelletier, *Physics of Collisional Plasmas*,
DOI 10.1007/978-94-007-4558-2,

The vector product is not commutative.

Note the important rule for the *double vector product*:

$$\boldsymbol{A} \wedge (\boldsymbol{B} \wedge \boldsymbol{C}) = (\boldsymbol{A} \cdot \boldsymbol{C})\boldsymbol{B} - (\boldsymbol{A} \cdot \boldsymbol{B})\boldsymbol{C} \ . \tag{VIII.4}$$

Tensor product of two vectors: $\boldsymbol{A} \otimes \boldsymbol{B}$

The result is a second-order tensor $\underline{\boldsymbol{T}}$, with its components T_{ij} being the algebraic product of the components A_i and B_j:

$$T_{ij} = A_i B_j \ . \tag{VIII.5}$$

It follows that:

$$\boldsymbol{A} \otimes \boldsymbol{B} = (\boldsymbol{B} \otimes \boldsymbol{A})^T \ . \tag{VIII.6}$$

The product is not commutative, unless the vectors are parallel. The superscript symbol T indicates that the tensor is transposed (T_{ij} becomes T_{ji}).

Remark: In the main text, for simplicity, we have represented the tensor product of two vectors $\boldsymbol{A}$ and $\boldsymbol{B}$ in the form $\boldsymbol{AB}$ rather than $\boldsymbol{A} \otimes \boldsymbol{B}$.

Product of two tensors

Consider two second-order tensors $\underline{\boldsymbol{S}}$ and $\underline{\boldsymbol{T}}$.

Tensor product: $\underline{\boldsymbol{S}} \otimes \underline{\boldsymbol{T}}$

The result is a 4^{th} order tensor:

$$\underline{\boldsymbol{S}} \otimes \underline{\boldsymbol{T}} = \underline{\underline{\boldsymbol{U}}} \tag{VIII.7}$$

whose components are:

$$U_{ijkl} = S_{ij} T_{kl} \ . \tag{VIII.8}$$

Singly-contracted product: $\underline{\boldsymbol{S}} \cdot \underline{\boldsymbol{T}}$

The result is a 2^{nd} order tensor:

$$\underline{\boldsymbol{S}} \cdot \underline{\boldsymbol{T}} = \underline{\boldsymbol{U}} \tag{VIII.9}$$

whose components are:

$$U_{ij} = \sum_k S_{ik} T_{kj} \tag{VIII.10}$$

and if both tensors are symmetric:

$$\underline{\boldsymbol{S}} \cdot \underline{\boldsymbol{T}} = (\underline{\boldsymbol{T}} \cdot \underline{\boldsymbol{S}})^T = (\underline{\boldsymbol{U}})^T = \underline{\boldsymbol{U}} \,. \tag{VIII.11}$$

Doubly-contracted product: $\underline{\boldsymbol{S}} : \underline{\boldsymbol{T}}$

The result is a scalar:

$$\underline{\boldsymbol{S}} : \underline{\boldsymbol{T}} = \sum_i \sum_j S_{ij} T_{ji} = U \tag{VIII.12}$$

with:

$$\underline{\boldsymbol{S}} : \underline{\boldsymbol{T}} = \underline{\boldsymbol{T}} : \underline{\boldsymbol{S}} \,. \tag{VIII.13}$$

Product between a vector and a tensor

Consider $\boldsymbol{A}$, a vector, and $\underline{\boldsymbol{T}}$, a second-order tensor.

Tensor product of a vector with a 2nd order tensor

The result is a 3rd order tensor:

$$\boldsymbol{A} \otimes \underline{\boldsymbol{T}} = \underline{\underline{\boldsymbol{Q}}} \tag{VIII.14}$$

whose components are:

$$Q_{ijk} = A_i T_{jk} \,. \tag{VIII.15}$$

Contracted product of a vector with a 2nd order tensor

The result is a vector:

$$\underline{\boldsymbol{T}} \cdot \boldsymbol{A} = \boldsymbol{D} \tag{VIII.16}$$

whose components are:

$$D_i = \sum_j T_{ij} A_j \,. \tag{VIII.17}$$

Similarly, the product $\boldsymbol{A} \cdot \underline{\boldsymbol{T}}$ is a vector:

$$\boldsymbol{A} \cdot \underline{\boldsymbol{T}} = \boldsymbol{D}' \tag{VIII.18}$$

whose components are:

$$D'_i = \sum_j A_j T_{ji} \,. \tag{VIII.19}$$

Thus, if $\underline{\boldsymbol{T}}$ is a symmetric tensor ($T_{ij} = T_{ji}$), the product is commutative:

$$\underline{\boldsymbol{T}} \cdot \boldsymbol{A} = \boldsymbol{A} \cdot \underline{\boldsymbol{T}} \,. \tag{VIII.20}$$

If $\underline{\boldsymbol{T}}$ is obtained from the tensor product of two vectors:

$$\underline{\boldsymbol{T}} = \boldsymbol{B} \otimes \boldsymbol{C} \tag{VIII.21}$$

then:

$$\boldsymbol{A} \cdot (\boldsymbol{B} \otimes \boldsymbol{C}) = \boldsymbol{D} \,, \tag{VIII.22}$$

with components:

$$D_i = \sum_j A_j B_j C_i = (\boldsymbol{A} \cdot \boldsymbol{B}) C_i \,, \tag{VIII.23}$$

from which:

$$\boldsymbol{D} = \boldsymbol{A} \cdot (\boldsymbol{B} \otimes \boldsymbol{C}) = (\boldsymbol{A} \cdot \boldsymbol{B}) \boldsymbol{C} \tag{VIII.24}$$

and since the product is commutative:

$$\boldsymbol{D} = (\boldsymbol{A} \otimes \boldsymbol{B}) \cdot \boldsymbol{C} = \boldsymbol{A} (\boldsymbol{B} \cdot \boldsymbol{C}) \,. \tag{VIII.25}$$

Contracted product of a vector with a 3rd order tensor

Consider $\underline{\underline{\boldsymbol{Q}}}$, a 3rd order tensor. The result is a 2nd order tensor $\underline{\boldsymbol{T}}$:

$$\boldsymbol{A} \cdot \underline{\underline{\boldsymbol{Q}}} = \underline{\boldsymbol{T}} \tag{VIII.26}$$

whose components are:

$$T_{ij} = \sum_k A_k Q_{kij} \,. \tag{VIII.27}$$

Similarly:

$$\underline{\underline{\boldsymbol{Q}}} \cdot \boldsymbol{A} = \underline{\boldsymbol{T}}' \tag{VIII.28}$$

is a 2nd order tensor whose components are:

$$T'_{ij} = \sum_k Q_{ijk} A_k \,. \tag{VIII.29}$$

Vector product of a vector with a 2nd order tensor

The result is a 2nd order tensor:

$$\boldsymbol{A} \wedge \underline{\boldsymbol{T}} = \underline{\boldsymbol{U}} \tag{VIII.30}$$

whose components are:

$$U_{ij} = A_{i+1}T_{i-1,j} - A_{i-1}T_{i+1,j} \; . \tag{VIII.31}$$

The vector column j of the tensor $\underline{\boldsymbol{U}}$ is the vector product of the vector $\boldsymbol{A}$ by the column vector j of the tensor $\underline{\boldsymbol{T}}$.

Operations involving the differential operator (Cartesian coordinates)

The differential operator $\boldsymbol{\nabla}$ (or $\partial/\partial\boldsymbol{r}$) can be considered as a vector, whose components in Cartesian coordinates are:

$$\boldsymbol{\nabla}_i = \frac{\partial}{\partial x_i} \; . \tag{VIII.32}$$

Divergence of a vector

The result is a scalar:

$$\boldsymbol{\nabla} \cdot \boldsymbol{A} = \sum_{i=1}^{3} \frac{\partial A_i}{\partial x_i} = C \; . \tag{VIII.33}$$

Divergence of a 2nd order tensor

The result is a vector:

$$\boldsymbol{\nabla} \cdot \underline{\boldsymbol{T}} = \boldsymbol{A} \tag{VIII.34}$$

whose components are:

$$A_i = \sum_j \frac{\partial T_{ji}}{\partial x_j} \; . \tag{VIII.35}$$

The divergence is the contracted product of the differential operator $\boldsymbol{\nabla}$ with a vector or a tensor.

Gradient of a scalar

The result is a vector:

$$\boldsymbol{\nabla} C = \boldsymbol{A} \tag{VIII.36}$$

whose components are:

$$A_i = \frac{\partial C}{\partial x_i} \; . \tag{VIII.37}$$

Gradient of a vector or a tensor

In general, the gradient is the tensor product of the differential operator $\boldsymbol{\nabla}$ with a scalar, a vector or a tensor.
Thus, operating on a vector $\boldsymbol{A}$, the result is a 2nd order tensor:

$$\boldsymbol{\nabla A} \equiv \boldsymbol{\nabla} \otimes \boldsymbol{A} = \underline{\boldsymbol{T}} \tag{VIII.38}$$

whose components are:

$$T_{ij} = \frac{\partial A_j}{\partial x_i} \, . \tag{VIII.39}$$

Note that $\boldsymbol{\nabla} B$ is a vector while $\boldsymbol{\nabla B}$ is a 2nd order tensor.

Curl of a vector

The curl is the vector product of the differential operator $\boldsymbol{\nabla}$ with a vector. We obtain a (pseudo) vector:

$$\boldsymbol{\nabla} \wedge \boldsymbol{A} = \boldsymbol{C} \tag{VIII.40}$$

with the components:

$$C_i = \frac{\partial A_{i-1}}{\partial x_{i+1}} - \frac{\partial A_{i+1}}{\partial x_{i-1}} \, . \tag{VIII.41}$$

Laplacian of a scalar

This is a scalar:

$$\Delta C = \sum_i \frac{\partial^2 C}{\partial x_i^2} \, . \tag{VIII.42}$$

Since:

$$\sum_i \frac{\partial^2 C}{\partial x_i^2} = \sum_i \frac{\partial}{\partial x_i} \left(\frac{\partial C}{\partial x_i} \right) = \boldsymbol{\nabla} \cdot (\boldsymbol{\nabla} C) \, , \tag{VIII.43}$$

thus:

$$\Delta C = \boldsymbol{\nabla} \cdot (\boldsymbol{\nabla} C) = \nabla^2 C \, . \tag{VIII.44}$$

Laplacian of a vector

This is a vector:

$$\Delta \boldsymbol{A} = \boldsymbol{C} \tag{VIII.45}$$

with the components:

$$C_i = \sum_j \frac{\partial^2 A_i}{\partial x_j^2} \, . \tag{VIII.46}$$

Since:

$$\Delta \boldsymbol{A} = \sum_j \frac{\partial^2 A_i}{\partial x_j^2} = \sum_j \frac{\partial}{\partial x_j} \left(\frac{\partial A_i}{\partial x_j} \right) = \boldsymbol{\nabla} \cdot (\boldsymbol{\nabla} \otimes \boldsymbol{A}) \, , \tag{VIII.47}$$

thus:

$$\Delta \boldsymbol{A} = \boldsymbol{\nabla} \cdot (\boldsymbol{\nabla} \otimes \boldsymbol{A}) = \nabla^2 \boldsymbol{A} \, . \tag{VIII.48}$$

Remark: One should not forget that $\boldsymbol{\nabla}$ is a differential operator, and that, as a consequence, when it is applied to a product, it is applied on each of the terms. For instance: $\boldsymbol{\nabla} \cdot (\boldsymbol{B} \otimes \boldsymbol{C}) = (\boldsymbol{\nabla} \cdot \boldsymbol{B})\boldsymbol{C} + (\boldsymbol{B} \cdot \boldsymbol{\nabla})\boldsymbol{C}$.

Appendix IX
Orientation of $\boldsymbol{w}_{2\perp}$ in the Reference Triad with Cartesian Axes $(\boldsymbol{E}_{0\perp} \wedge \boldsymbol{B}, \boldsymbol{E}_{0\perp}, \boldsymbol{B})$

We will make use of the reference triad shown in Fig. 2.8 and of the representation of the velocity $\boldsymbol{w}_{2\perp}$ in Fig. 2.9. From (2.137), for an electron ($q = -e$ and $\omega_c = \omega_{ce}$), we then have:

$$\boldsymbol{w}_{2\perp} = -\frac{e}{m_e(\omega_{ce}^2 - \omega^2)} \left\{ i\omega \boldsymbol{E}_{0\perp} - \frac{\omega_{ce}}{B}(\boldsymbol{E}_{0\perp} \wedge \boldsymbol{B}) \right\} \mathrm{e}^{\mathrm{i}\omega t} \tag{IX.1}$$

1. The case $\omega > \omega_{ce}$: major axis along $\boldsymbol{E}_{0\perp}$
   From (IX.1), we have:

$$\begin{aligned} \Re(\boldsymbol{w}_{2\perp}) = \frac{e}{m_e(\omega^2 - \omega_{ce}^2)} \Re\Big\{ & \mathrm{i}\omega(\cos\omega t + \mathrm{i}\sin\omega t)\boldsymbol{E}_{0\perp} \\ & - \frac{\omega_{ce}}{B}(\cos\omega t + \mathrm{i}\sin\omega t)(\boldsymbol{E}_{0\perp} \wedge \boldsymbol{B}) \Big\} \\ = -A_1\omega(\sin\omega t)\boldsymbol{E}_{0\perp} & - A_2\omega_{ce}(\cos\omega t)(\boldsymbol{E}_{0\perp} \wedge \boldsymbol{B}) \end{aligned} \tag{IX.2}$$

   where A_1 and A_2 are constants.
   At $t = 0$, we have $\boldsymbol{E}_\perp = \boldsymbol{E}_{0\perp}$, $\boldsymbol{w}_{2\perp} = -A_2\omega_{ce}(\boldsymbol{E}_{0\perp} \wedge \boldsymbol{B})$ and at $t = \mathcal{T}/2$, $\boldsymbol{E}_\perp = -\boldsymbol{E}_{0\perp}$, $\boldsymbol{w}_{2\perp} = A_2\omega_{ce}(\boldsymbol{E}_{0\perp} \wedge \boldsymbol{B})$, as shown in Fig. 2.9.

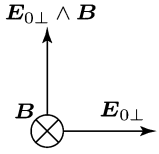

2. The case $\omega < \omega_{ce}$: major axis along $\boldsymbol{E}_{0\perp} \wedge \boldsymbol{B}$
   From (IX.1), we have:

$$\Re(\boldsymbol{w}_{2\perp}) = A_1\omega(\sin\omega t)\boldsymbol{E}_{0\perp} + A_2\omega_{ce}(\cos\omega t)(\boldsymbol{E}_{0\perp} \wedge \boldsymbol{B})\ . \tag{IX.3}$$

   At $t = 0$, we have $\boldsymbol{E}_\perp = \boldsymbol{E}_{0\perp}$, $\boldsymbol{w}_{2\perp} = A_2\omega_{ce}(\boldsymbol{E}_{0\perp} \wedge \boldsymbol{B})$ and at $t = \mathcal{T}/2$, $\boldsymbol{E}_\perp = -\boldsymbol{E}_{0\perp}$, $\boldsymbol{w}_{2\perp} = -A_2\omega_{ce}(\boldsymbol{E}_{0\perp} \wedge \boldsymbol{B})$ (Fig. 2.9). Note that, in the present case, the velocity is out of phase by a factor π with respect to the case $\omega > \omega_{ce}$.

M. Moisan, J. Pelletier, *Physics of Collisional Plasmas*,
DOI 10.1007/978-94-007-4558-2,

Appendix X
Force Acting on a Charged Particle in the Direction of a Magnetic Field $\boldsymbol{B}$ Weakly Non-uniform Axially: Variant of (2.177)

The Lorentz force due to $\boldsymbol{B}$ along the z axis can be written $F_z = q(\boldsymbol{w}\wedge\boldsymbol{B})\cdot\hat{\mathbf{e}}_z$. In cylindrical coordinates, due to the helical motion (components along $\hat{\mathbf{e}}_z$ and $\hat{\mathbf{e}}_\varphi$), we have:

$$\boldsymbol{w}\wedge\boldsymbol{B} = \begin{vmatrix} \hat{\mathbf{e}}_r & \hat{\mathbf{e}}_\varphi & \hat{\mathbf{e}}_z \\ 0 & w_\perp & w_\parallel \\ B_r & 0 & B_z \end{vmatrix} . \tag{X.1}$$

This leads to:

$$F_z = -qw_\perp B_r . \tag{X.2}$$

However, we also know that close enough to the axis of symmetry of the field $\boldsymbol{B}$, we can write:

$$rB_r \approx -\int_0^r r' \left(\frac{\partial B_z}{\partial z}\right)_{r'=0} \mathrm{d}r' = -\frac{1}{2} r^2 \left(\frac{\partial B_z}{\partial z}\right)_{r=0} . \tag{2.161}$$

Assuming that the particle moves about the guiding centre, defined by the axis of symmetry of the field $\boldsymbol{B}$, with a Larmor radius r_B, we can then set $r = r_B$ in the expression for B_r, from which:

$$F_z = qw_\perp \frac{r_B}{2}\frac{\partial B_z}{\partial z} \tag{X.3}$$

and

$$\begin{aligned} F_z &= qw_\perp \frac{w_\perp}{2\omega_c}\frac{\partial B_z}{\partial z} = q\frac{w_\perp^2}{2}\left(\frac{m_\alpha}{-qB_z}\right)\frac{\partial B_z}{\partial z} \\ &= -\frac{1}{2}\frac{m_\alpha w_\perp^2}{B_z}\frac{\partial B_z}{\partial z} = -\mu\left(\frac{\partial B_z}{\partial z}\right) \end{aligned} \tag{2.177}$$

since $\mu = \mathcal{E}_{\mathrm{kin}\perp}/B_z$ (2.148).

The axial non uniformity of the field $\boldsymbol{B}$ gives rise to a force proportional to the gradient of the field.

M. Moisan, J. Pelletier, *Physics of Collisional Plasmas*,
DOI 10.1007/978-94-007-4558-2,

Appendix XI
The Magnetic Moment, an Invariant in the Guiding Centre Approximation

We will consider the case where there is no applied electric field $\boldsymbol{E}$. We will also neglect the field $\boldsymbol{E}$ induced by the inhomogeneity of $\boldsymbol{B}$ in the frame of the particle: this is consistent with the zero-order guiding centre approximation. Under these conditions, the total particle kinetic energy, $W_T = W_\perp + W_\parallel$ is constant (2.179). It follows that:

$$\frac{\mathrm{d}}{\mathrm{d}t}(W_\parallel) \equiv \frac{\mathrm{d}}{\mathrm{d}t}\left(\frac{1}{2}m_\alpha w_z^2\right) = -\frac{\mathrm{d}}{\mathrm{d}t}(W_\perp) \tag{XI.1}$$

and, furthermore:

$$\frac{\mathrm{d}}{\mathrm{d}t}(W_\perp) \equiv \frac{\mathrm{d}}{\mathrm{d}t}\left(\frac{W_\perp B}{B}\right) = \frac{W_\perp}{B}\frac{\mathrm{d}B}{\mathrm{d}t} + B\frac{\mathrm{d}}{\mathrm{d}t}\left(\frac{W_\perp}{B}\right) . \tag{XI.2}$$

Knowing that:

$$F_z = -\mu\frac{\partial B_z}{\partial z} , \tag{2.177}$$

by multiplying each side of (2.177) by w_z, and since $\mu = \dfrac{W_\perp}{B}$:

$$w_z m_\alpha \frac{\mathrm{d}w_z}{\mathrm{d}t} \equiv \frac{\mathrm{d}}{\mathrm{d}t}\left(\frac{1}{2}m_\alpha w_\parallel^2\right) = -\frac{W_\perp}{B}\frac{\partial B_z}{\partial z}\frac{\mathrm{d}z}{\mathrm{d}t} = -\frac{W_\perp}{B}\frac{\mathrm{d}B_z}{\mathrm{d}t} , \tag{XI.3}$$

then, applying (XI.1), the LHS of (XI.3) can be written:

$$-\frac{\mathrm{d}}{\mathrm{d}t}\left(\frac{1}{2}m_\alpha w_\perp^2\right) = -\frac{W_\perp}{B}\frac{\mathrm{d}B_z}{\mathrm{d}t} . \tag{XI.4}$$

Taking account of (XI.2) and replacing the LHS of equation (XI.4) leads to:

$$\frac{W_\perp}{B}\frac{\mathrm{d}B_z}{\mathrm{d}t} + B\frac{\mathrm{d}}{\mathrm{d}t}\left(\frac{W_\perp}{B}\right) = \frac{W_\perp}{B}\frac{\mathrm{d}B_z}{\mathrm{d}t} , \tag{XI.5}$$

M. Moisan, J. Pelletier, *Physics of Collisional Plasmas*,
DOI 10.1007/978-94-007-4558-2,

which clearly imposes that:

$$\frac{\mathrm{d}}{\mathrm{d}t}\left(\frac{W_\perp}{B}\right) \equiv \frac{\mathrm{d}\mu}{\mathrm{d}t} = 0\,, \tag{XI.6}$$

i.e. the magnetic moment μ is independent of t. We obtained the same result in the introduction of Sect. 2.2.3 (p. 137).

Appendix XII
Drift Velocity $\boldsymbol{w}_d$ of a Charged Particle Subjected to an Arbitrary Force $\boldsymbol{F}_d$ in a Field $\boldsymbol{B}$: the Magnetic Field Drift

Generalisation of the expression for the drift velocity in a field $\boldsymbol{B}$ from the expression for the electric field drift

For the electric field drift, we found (2.114):

$$\boldsymbol{w}_{de} = \frac{\boldsymbol{E}_\perp \wedge \boldsymbol{B}}{B^2} \ , \tag{XII.1}$$

which is an expression that can be generalised by setting $q\boldsymbol{E}_\perp = \boldsymbol{F}_{de}$, where the meaning of $\boldsymbol{F}_{de}$ can be extended to include an arbitrary force $\boldsymbol{F}_d$, which leads us to the general expression:

$$\boldsymbol{w}_d = \frac{\boldsymbol{F}_d \wedge \boldsymbol{B}}{qB^2} \ . \tag{XII.2}$$

Application to the case of the magnetic field drift (rectilinear field lines) in a weakly inhomogeneous field $\boldsymbol{B}$

Since the field $\boldsymbol{B}$ is weakly inhomogeneous, to zeroth order μ is a constant of the motion and, following (2.177), which we generalise in three dimensions by writing:

$$\boldsymbol{F}_{dm} = \boldsymbol{\mu} \cdot \boldsymbol{\nabla} \boldsymbol{B} \ . \tag{XII.3}$$

In the case of rectilinear magnetic field lines, let $\boldsymbol{B}$ be directed along $\hat{\mathbf{e}}_z$ and the inhomogeneity along y; then $\boldsymbol{\mu}$, which is connected to the diamagnetic field, is directed along $-\hat{\mathbf{e}}_z$:

$$\boldsymbol{\mu} = -\mu_z \hat{\mathbf{e}}_z \quad \text{and} \quad \boldsymbol{B} = B_z(y)\hat{\mathbf{e}}_z \ , \tag{XII.4}$$

M. Moisan, J. Pelletier, *Physics of Collisional Plasmas*,
DOI 10.1007/978-94-007-4558-2,

we then have:

$$\boldsymbol{F}_{dm} \equiv -\mu_z \hat{\mathbf{e}}_z \cdot \left(\frac{\partial B_z}{\partial y} \hat{\mathbf{e}}_y \hat{\mathbf{e}}_z \right) = -\mu_z \frac{\partial B_z}{\partial y} \hat{\mathbf{e}}_y \ . \tag{XII.5}$$

Substituting the expression for the force generating the magnetic-field drift (XII.5) in (XII.2), we obtain:

$$\boldsymbol{w}_{dm} \equiv -\mu_z \frac{\partial B_z}{\partial y} \frac{\hat{\mathbf{e}}_y \wedge B \hat{\mathbf{e}}_z}{qB^2} = \frac{\mu}{q} \frac{(\boldsymbol{B} \wedge \boldsymbol{\nabla} B)}{B^2} \ , \tag{XII.6}$$

which is exactly the same equation we obtained in (2.217): this result supports our hypothesis that (XII.2) is valid for an arbitrary force $\boldsymbol{F}_d$.

Appendix XIII
Magnetic-Field Drift Velocity $\boldsymbol{w}_{dm}$ in the Frenet Frame Associated with the Lines of Force of a Magnetic Field with Weak Curvature

To first order, the particle follows a cyclotron motion around a line of force, which constitutes the axis of its helical motion.

Frenet-(Serret) frame

At each point on a magnetic field line of force (Fig. XIII.1), we can construct a Cartesian frame such that:

1. The unit vector $\hat{\mathbf{e}}_z$ is directed along the **tangent** to the magnetic field line of $\boldsymbol{B}$ at each point,
2. $\hat{\mathbf{e}}_y$ is **normal** to this tangent, and directed along the *radius of curvature* $\boldsymbol{\rho}$[187], this second vector pointing towards the field line, i.e. in the opposite direction to $\hat{\mathbf{e}}_y$, and
3. $\hat{\mathbf{e}}_x$ is along the **binormal**, i.e. in the direction perpendicular to the two other unit vectors, such as to form a right-handed triad.

The Frenet frame is also, to a first approximation, the *natural frame of the particle* in the present case.

Frenet relations

Classical mechanics teaches us that on a trajectory s connected to a Frenet frame:

$$\frac{\mathrm{d}\hat{\mathbf{e}}_z}{\mathrm{d}s} = \frac{\hat{\mathbf{e}}_y}{\rho} = -\frac{\boldsymbol{\rho}}{\rho^2}\,, \tag{XIII.1}$$

[187] The radius of curvature at a point A on a curve is the distance between that point and the intersection of two normals to the curve, situated immediately on either side of the point A.

M. Moisan, J. Pelletier, *Physics of Collisional Plasmas*,
DOI 10.1007/978-94-007-4558-2,

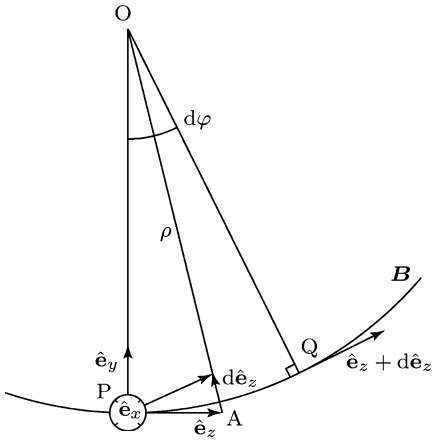

Fig. XIII.1 A Frenet frame, constructed on a magnetic field line with radius of curvature $\boldsymbol{\rho}$. The unit vector $\hat{\mathbf{e}}_x$ is directed into the page. The unit vector $\hat{\mathbf{e}}_z + \mathrm{d}\hat{\mathbf{e}}_z$, at point Q is transported, in parallel, to the point P in order to show the direction of $\mathrm{d}\hat{\mathbf{e}}_z$.

where the radius of curvature ρ is obtained from the derivative of the local tangents, as suggested in Fig. XIII.1. In the case where $y(z)$ describes the line of force, one can show that, provided $\mathrm{d}y/\mathrm{d}z$ is not too large:

$$\frac{\mathrm{d}^2 y}{\mathrm{d}z^2} = \frac{1}{\rho} \,. \tag{XIII.2}$$

Further, the components of the vector $\boldsymbol{\rho}$ can be written (Jancel and Kahan):

$$\frac{\rho_x}{\rho^2} = -\frac{1}{B}\frac{\partial B_x}{\partial z} \,, \tag{XIII.3}$$

$$\frac{\rho_y}{\rho^2} = -\frac{1}{B}\frac{\partial B_y}{\partial z} \,, \tag{XIII.4}$$

$$\frac{\rho_z}{\rho^2} = 0 \,. \tag{XIII.5}$$

Components of $\boldsymbol{\nabla B}$

The Maxwell equation $\boldsymbol{\nabla} \wedge \boldsymbol{B} = 0$ (without the RHS, in the framework of individual particle trajectories[85]) leads to:

$$\hat{\mathbf{e}}_x \left(\frac{\partial B_z}{\partial y} - \frac{\partial B_y}{\partial z} \right) + \hat{\mathbf{e}}_y \left(\frac{\partial B_x}{\partial z} - \frac{\partial B_z}{\partial x} \right) + \hat{\mathbf{e}}_z \left(\frac{\partial B_y}{\partial x} - \frac{\partial B_x}{\partial y} \right) = 0 \,. \tag{XIII.6}$$

Further, from the assumption that the inhomogeneity in $\boldsymbol{B}$ is independent of y, we have $\dfrac{\partial B_z}{\partial y} \neq 0$, such that (XIII.6) requires:

$$\frac{\partial B_z}{\partial y} = \frac{\partial B_y}{\partial z} \,. \tag{XIII.7}$$

The other terms in (XIII.6) are zero. Equations (XIII.3) and (XIII.4) then become:

$$\rho_x = 0 \,, \tag{XIII.8}$$

$$\frac{\rho_y}{\rho^2} = -\frac{1}{B_z}\frac{\partial B_z}{\partial y} \,, \tag{XIII.9}$$

such that $\rho_y = \rho$.

Parameterisation of a curved field line

In our case, $\boldsymbol{B} = B_z\hat{\mathbf{e}}_z + B_y\hat{\mathbf{e}}_y$, where $|B_y| \ll |B_z|$ is a first order correction to B_z, provided the curvature of the field is not too large. We are seeking a relation $y(z)$ to characterise this line of force.

We can perform a limited Taylor series development of the component B_y, with $B_y(0) = 0$, since this quantity is of order one, and:

$$B_y \approx \frac{\partial B_y}{\partial x}\,\mathrm{d}x + \frac{\partial B_y}{\partial y}\,\mathrm{d}y + \frac{\partial B_y}{\partial z}\,\mathrm{d}z \,, \tag{XIII.10}$$

where, according to (XIII.6) and (XIII.7), only the component $\dfrac{\partial B_y}{\partial z}$ is non zero, so that:

$$B_y \approx \frac{\partial B_y}{\partial z}\,\mathrm{d}z \,, \tag{XIII.11}$$

which, from (XIII.7), becomes:

$$B_y \simeq \frac{\partial B_z}{\partial y}\mathrm{d}z \,, \tag{XIII.12}$$

hence, for z small, from (2.221):

$$B_y \simeq B_0\beta z \,. \tag{XIII.13}$$

Further, by definition, locally (see Fig. 2.17):

$$\frac{B_y}{B_z} = \frac{\mathrm{d}y}{\mathrm{d}z} \,, \tag{XIII.14}$$

where:

$$\frac{B_y}{B_z} = \frac{B_0\beta z}{B_0(1+\beta y)} \simeq \beta z \,, \tag{XIII.15}$$

hence:

$$\frac{\mathrm{d}y}{\mathrm{d}z} = \beta z \,. \tag{XIII.16}$$

Integrating (XIII.2), we have (since $y = 0$ at $z = 0$):

$$\frac{\mathrm{d}y}{\mathrm{d}z} = \frac{z}{\rho} \,, \tag{XIII.17}$$

so we can deduce that:

$$\beta \approx 1/\rho \,. \tag{XIII.18}$$

The equation for $\boldsymbol{w_{dm}}$ in the Frenet frame

We have already shown that:

$$\boldsymbol{w}_{dm} = m_\alpha \frac{w_\perp^2}{2} \frac{1}{q_\alpha B^3} (\boldsymbol{B} \wedge \boldsymbol{\nabla} B) \,. \tag{2.216}$$

If we now set $\omega_c = -q_\alpha B/m_\alpha$, this can be written explicitly:

$$\boldsymbol{w}_{dm} = -\frac{1}{\omega_c B^2} \frac{w_\perp^2}{2} \left(\boldsymbol{B} \wedge \frac{\partial B_z}{\partial y} \hat{\mathbf{e}}_y \right) \,. \tag{XIII.19}$$

From (2.221) and (XIII.18), we obtain:

$$\frac{\partial B_z}{\partial y} = \frac{B_z}{\rho} \,, \tag{XIII.20}$$

and from (XIII.15):

$$\boldsymbol{w}_{dm} = \frac{1}{\omega_c B^2} \frac{w_\perp^2}{2} \left(\frac{B_z}{\rho} \hat{\mathbf{e}}_y \wedge \boldsymbol{B} \right) \,. \tag{XIII.21}$$

By introducing $\boldsymbol{\rho}$, directed opposite to $\hat{\mathbf{e}}_y$, we finally arrive at:

$$\boldsymbol{w}_{dm} = -\frac{1}{\omega_c B} \frac{w_\perp^2}{2} \left(\frac{\boldsymbol{\rho}}{\rho^2} \wedge \boldsymbol{B} \right) \,. \tag{XIII.22}$$

This expression, in contrast to (2.216), includes the (weak) curvature of the field lines.

Appendix XIV
Spherical Harmonics

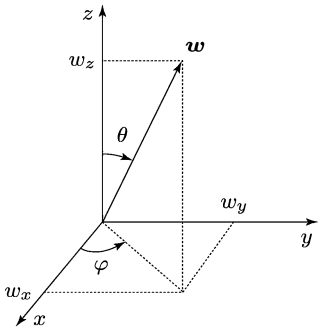

Fig. XIV.1 Spherical coordinate system in velocity space.

If the velocity $\boldsymbol{w}$ is expressed in spherical coordinates, the electron distribution function can be developed in *spherical harmonics*:

$$C_{lm} = w^l P_{lm}(\cos\theta)\cos m\varphi \,, \tag{XIV.1}$$

$$S_{lm} = w^l P_{lm}(\cos\theta)\sin m\varphi \,, \tag{XIV.2}$$

where $P_{lm}(\cos\theta)$ is the m^{th} order *Legendre function*, defined for $l \geq 1$ and $0 \leq m \leq l$ by:

$$P_{lm}(\mu) = (1-\mu^2)^{\frac{m}{2}} \frac{\mathrm{d}^m}{\mathrm{d}\mu^m} P_l(\mu) \,, \tag{XIV.3}$$

and P_l is the Legendre *polynomial* of degree l. Note that for $m = 0$,

$$P_{lm}(\mu) = P_l(\mu) \,. \tag{XIV.4}$$

The first Legendre polynomials $P_{lm}(\mu)$ are:

M. Moisan, J. Pelletier, *Physics of Collisional Plasmas*,
DOI 10.1007/978-94-007-4558-2,

$$P_0(\mu) = 1\ , \quad P_1(\mu) = \mu\ , \quad P_{11}(\mu) = (1-\mu^2)^{\frac{1}{2}}\ ,$$
$$P_2(\mu) = \frac{1}{2}\left(3\mu^2 - 1\right)\ , \quad P_{21}(\mu) = 3\mu(1-\mu^2)^{\frac{1}{2}}\ , \quad P_{22}(\mu) = 3(1-\mu^2)\ ,$$
$$P_3(\mu) = \frac{1}{2}\left(5\mu^3 - 3\mu\right)\ \ldots \tag{XIV.5}$$

The first spherical functions, for $\mu = \cos\theta$, are therefore:

$$C_{00} = 1\ , \quad C_{10} = w\cos\theta = w_z\ , \quad C_{11} = w\sin\theta\cos\varphi = w_x\ ,$$
$$S_{11} = w\sin\theta\sin\varphi = w_y\ , \quad C_{20} = w^2\left(\frac{3\cos^2\theta - 1}{2}\right)\ . \tag{XIV.6}$$

Assuming that the system is symmetrical in φ, the distribution function $f(\boldsymbol{r},\ \boldsymbol{w},\ t)$ can be expanded in terms of C_{i0} yielding:

$$f(\boldsymbol{r}, \boldsymbol{w}, t) =$$
$$f_0(\boldsymbol{r}, w, t) + f_1(\boldsymbol{r}, w, t)\cos\theta + f_2(\boldsymbol{r}, w, t)\left(\frac{3\cos^2\theta - 1}{2}\right) + \ldots \tag{3.18}$$

Appendix XV
Expressions for the Terms $\underline{\boldsymbol{M}}$ and $\underline{\boldsymbol{\mathcal{R}}}_{\boldsymbol{\alpha}}$ in the Kinetic Pressure Transport Equation (3.155)

Relationship between $\underline{\boldsymbol{M}}$ and the magnetic force

To calculate $\underline{\boldsymbol{M}}$ from (3.155) when the particles α are subjected to a magnetic field $\boldsymbol{B}$ (Laplace force[90]), it is sufficient to write (VIII.31):

$$M_{ij} = n_\alpha q_\alpha \langle (w_{i+1}B_{i-1} - w_{i-1}B_{i+1})u_j + (w_{j+1}B_{j-1} - w_{j-1}B_{j+1})u_i \rangle \ . \tag{XV.1}$$

Reordering the terms, we obtain:

$$\begin{aligned} M_{ij} = {} & n_\alpha q_\alpha \langle (u_{i+1} + v_{i+1})B_{i-1}u_j - (u_{i-1} + v_{i-1})B_{i+1}u_j \rangle \\ & + n_\alpha q_\alpha \langle (u_{j+1} + v_{j+1})B_{j-1}u_i - (u_{j-1} + v_{j-1})B_{j+1}u_i \rangle \ , \end{aligned} \tag{XV.2}$$

hence:

$$\begin{aligned} M_{ij} = {} & \frac{q_\alpha}{m_\alpha} \left[B_{i-1}\Psi_{i+1,\ j} - B_{i+1}\Psi_{i-1,\ j} \right] \\ & + \frac{q_\alpha}{m_\alpha} \left[B_{j-1}\Psi_{j+1,\ i} - B_{j+1}\Psi_{j-1,\ i} \right] \ , \end{aligned} \tag{XV.3}$$

which can be written in tensor form (VIII.6):

$$\underline{\boldsymbol{M}} = -\frac{q_\alpha}{m_\alpha} \left[\boldsymbol{B} \wedge \underline{\boldsymbol{\Psi}} + (\boldsymbol{B} \wedge \underline{\boldsymbol{\Psi}})^T \right] \ . \tag{XV.4}$$

Expression for the collision tensor $\underline{\boldsymbol{\mathcal{R}}}_{\boldsymbol{\alpha}}$

Recall that:

$$\underline{\boldsymbol{\mathcal{R}}}_\alpha = \sum_{\beta \neq \alpha} \underline{\boldsymbol{\mathcal{R}}}_{\alpha\beta} \tag{3.141}$$

where:

M. Moisan, J. Pelletier, *Physics of Collisional Plasmas*,
DOI 10.1007/978-94-007-4558-2,

$$\underline{\boldsymbol{\mathcal{R}}}_{\alpha\beta} = \int m_\alpha(\boldsymbol{w}_\alpha - \boldsymbol{v}_\alpha)(\boldsymbol{w}_\alpha - \boldsymbol{v}_\alpha)S(f_\alpha)_\beta \,\mathrm{d}\boldsymbol{w}_\alpha \,. \tag{XV.5}$$

The tensor $\underline{\boldsymbol{\mathcal{R}}}_{\alpha\beta}$ can be written, after expansion:

$$\underline{\boldsymbol{\mathcal{R}}}_{\alpha\beta} = \int m_\alpha(\boldsymbol{w}_\alpha\boldsymbol{w}_\alpha - \boldsymbol{v}_\alpha\boldsymbol{w}_\alpha - \boldsymbol{w}_\alpha\boldsymbol{v}_\alpha + \boldsymbol{v}_\alpha\boldsymbol{v}_\alpha)S(f_\alpha)_\beta \,\mathrm{d}\boldsymbol{w}_\alpha \,, \tag{XV.6}$$

hence:

$$\begin{aligned}\underline{\boldsymbol{\mathcal{R}}}_{\alpha\beta} = {} & \int m_\alpha(\boldsymbol{w}_\alpha\boldsymbol{w}_\alpha)S(f_\alpha)_\beta \,\mathrm{d}\boldsymbol{w}_\alpha - \boldsymbol{v}_\alpha \int m_\alpha\boldsymbol{w}_\alpha S(f_\alpha)_\beta \,\mathrm{d}\boldsymbol{w}_\alpha \\ & - \left[\boldsymbol{v}_\alpha \int m_\alpha\boldsymbol{w}_\alpha S(f_\alpha)_\beta \,\mathrm{d}\boldsymbol{w}_\alpha\right]^T + \boldsymbol{v}_\alpha\boldsymbol{v}_\alpha \int m_\alpha S(f_\alpha)_\beta \,\mathrm{d}\boldsymbol{w}_\alpha \,.\end{aligned} \tag{XV.7}$$

If the number of particles is conserved during collisions, the last term in (XV.7) is zero. Including (3.120), which defines $\boldsymbol{\mathcal{P}}_{\alpha\beta}$ (XV.7), we obtain the final form:

$$\underline{\boldsymbol{\mathcal{R}}}_{\alpha\beta} = \int m_\alpha\boldsymbol{w}_\alpha\boldsymbol{w}_\alpha S(f_\alpha)_\beta \,\mathrm{d}\boldsymbol{w}_\alpha - \boldsymbol{v}_\alpha\boldsymbol{\mathcal{P}}_{\alpha\beta} - [\boldsymbol{v}_\alpha\boldsymbol{\mathcal{P}}_{\alpha\beta}]^T \,. \tag{XV.8}$$

Appendix XVI
Closure of the Hydrodynamic Transport Equation for Kinetic Pressure in the Case of Adiabatic Compression

We will consider the transport equation for kinetic pressure $\underline{\underline{\boldsymbol{\Psi}}}$ (3.160), with the assumption of adiabatic compression (see main text): $\boldsymbol{\nabla} \cdot \underline{\underline{\boldsymbol{Q}}} = \underline{\underline{\mathbf{0}}}$ and $\underline{\underline{\boldsymbol{\mathcal{R}}}} = \underline{\underline{\mathbf{0}}}$. The equation then simplifies to give:

$$n \frac{\mathrm{d}}{\mathrm{d}t} \left(\frac{\underline{\underline{\boldsymbol{\Psi}}}}{n} \right) + \left(\underline{\underline{\boldsymbol{\Psi}}} \cdot \boldsymbol{\nabla} \right) \boldsymbol{v} + \left[\left(\underline{\underline{\boldsymbol{\Psi}}} \cdot \boldsymbol{\nabla} \right) \boldsymbol{v} \right]^T - \underline{\underline{\boldsymbol{M}}} = \underline{\underline{\mathbf{0}}} \, . \tag{XVI.1}$$

The structure of the tensor $\underline{\underline{\boldsymbol{M}}}$ (XV.2) is such that the off-diagonal terms are zero.

The equation (XVI.1), comprising second-order tensors, can lead to a scalar solution if we apply a contraction (Appendix VII) on the two indices of the various 2nd order tensors in the equation. Since a tensor $\underline{\underline{\boldsymbol{A}}}$ can be expressed as $\underline{\underline{\boldsymbol{A}}} = \hat{\mathbf{e}}_i \hat{\mathbf{e}}_j A_{ij}$, contracting the two indices ($i = j$) is equivalent to calculating the trace of $\underline{\underline{\boldsymbol{A}}}$. The result of such a contraction on indices of the same variance (subscripts here) leads to a scalar, provided the coordinate systems considered are Cartesian.

Taking account of (3.115), the value of the trace Tr of the first term of (XVI.1) is:

$$\mathrm{Tr} \left[n \frac{\mathrm{d}}{\mathrm{d}t} \frac{\underline{\underline{\boldsymbol{\Psi}}}}{n} \right] = n \frac{\mathrm{d}}{\mathrm{d}t} \frac{3p}{n} \, , \tag{XVI.2}$$

while the traces of the second and third terms give:

$$\mathrm{Tr} \left[\left(\underline{\underline{\boldsymbol{\Psi}}} \cdot \boldsymbol{\nabla} \right) \boldsymbol{v} \right] + \mathrm{Tr} \left[\left(\underline{\underline{\boldsymbol{\Psi}}} \cdot \boldsymbol{\nabla} \right) \boldsymbol{v} \right]^T = 2p \boldsymbol{\nabla} \cdot \boldsymbol{v} \, , \tag{XVI.3}$$

where we have set $\underline{\underline{\boldsymbol{\Psi}}} = n k_B T (\underline{\underline{\boldsymbol{I}}})$ (as in the warm plasma approximation). Finally, the complete trace of (XVI.1) is given by:

$$n \frac{\mathrm{d}}{\mathrm{d}t} \frac{3}{2} \frac{p}{n} + p \boldsymbol{\nabla} \cdot \boldsymbol{v} = 0 \, . \tag{XVI.4}$$

This scalar equation thus replaces a 2nd order tensor equation, for which closure has been achieved by setting $\boldsymbol{\nabla} \cdot \underline{\underline{\boldsymbol{Q}}} = \underline{\underline{\mathbf{0}}}$.

M. Moisan, J. Pelletier, *Physics of Collisional Plasmas*,
DOI 10.1007/978-94-007-4558-2,

Appendix XVII
Complementary Calculations to the Expression for $T_e(pR)$ (Sect. 3.13)

Maxwellian velocity distribution function expressed in terms of energy (eV)[188]

The following expression for the distribution function:

$$f(w) = \left(\frac{m_e}{2\pi k_B T_e}\right)^{\frac{3}{2}} \exp\left(-\frac{w^2}{v_{th}^2}\right) , \tag{3.293}$$

by its scalar velocity dependence, emphasises that we have neglected the anisotropy induced by the external field $\boldsymbol{E}$.

Introducing U_{eV}, the microscopic electron energy, expressed in eV:

$$U_{eV} = \frac{m_e w^2}{2e} , \tag{3.294}$$

we obtain:

$$w = \sqrt{\frac{2eU_{eV}}{m_e}} \tag{3.295}$$

[188] Substitution of the energy U_{eV} for w in $f(w)$ (isotropic) leads to the function $f(U_{eV})$, which is referred to as the *velocity distribution function expressed in terms of energy*. By the same token, we define an *energy distribution function* $F(U_{eV})$, by setting:

$$F(U_{eV}) U_{eV}^{\frac{1}{2}} \, \mathrm{d}U_{eV} = f(w) 4\pi w^2 \, \mathrm{d}w \, .$$

Thus, we have $F(U_{eV}) = 4\sqrt{2}\pi (e/m_e)^{3/2} f(w)$, hence:

$$F(U_{eV}) = \frac{2}{\pi^{\frac{1}{2}} (k_B T_e)^{\frac{3}{2}}} \exp\left(-\frac{eU_{eV}}{k_B T_e}\right) ,$$

the normalisation condition being:

$$\int_0^\infty F(U_{eV}) U_{eV}^{\frac{1}{2}} \, \mathrm{d}U_{eV} = 1 \, .$$

M. Moisan, J. Pelletier, *Physics of Collisional Plasmas*,
DOI 10.1007/978-94-007-4558-2,

and since:

$$\frac{1}{2}m_e v_{th}^2 = k_B T_e = \frac{2}{3}\left(\frac{3}{2}k_B T_e\right) = \frac{2}{3}e\bar{U}_{eV} \ , \tag{XVII.1}$$

where $\bar{U}_{eV} = 3k_B T_e/2e$ is the electron mean energy, we finally have:

$$v_{th} = \sqrt{\frac{4}{3}\frac{e}{m_e}\bar{U}_{eV}} \ . \tag{3.297}$$

After substitution in (3.293), we obtain:

$$f\left(\sqrt{\frac{2eU_{eV}}{m_e}}\right) = \frac{1}{(2\pi)^{\frac{3}{2}}}\left(\frac{3m_e}{2e\bar{U}_{eV}}\right)^{\frac{3}{2}} \exp\left(-\frac{2eU_{eV}}{m_e} \Big/ \frac{4e\bar{U}_{eV}}{3m_e}\right) \ , \tag{XVII.2}$$

where:

$$f\left(\sqrt{\frac{2eU_{eV}}{m_e}}\right) = \left(\frac{3}{4\pi}\frac{m_e}{e}\right)^{\frac{3}{2}} \frac{1}{\bar{U}_{eV}^{\frac{3}{2}}} \exp\left(-\frac{3}{2}\frac{U_{eV}}{\bar{U}_{eV}}\right) \ . \tag{3.298}$$

The ionisation frequency in terms of the reduced energies $\mathcal{U}$ and $\mathcal{U}_i$

As a starting point, we have equation (3.301)

$$\langle \nu_i \rangle = 3\sqrt{\frac{3e}{m_e\pi}}\,\frac{p_0}{\bar{U}_{eV}^{\frac{3}{2}}}\,a_{i0}\int_{\mathcal{E}_i}^{\infty}(U_{eV}-\mathcal{E}_i)\,U_{eV}\,\exp\left(-\frac{3}{2}\frac{U_{eV}}{\bar{U}_{eV}}\right)\mathrm{d}U_{eV} \ . \tag{3.301}$$

Introducing the change of variable required for the energies to be normalised to the average energy (so-called *reduced energies*):

$$\frac{3}{2}\frac{U_{eV}}{\bar{U}_{eV}} = \mathcal{U} \ , \qquad \frac{3}{2}\frac{\mathcal{E}_i}{\bar{U}_{eV}} = \mathcal{U}_i \ , \tag{3.302}$$

it follows that:

$$\langle \nu_i \rangle = 3\sqrt{\frac{3e}{m_e\pi}}\,\frac{p_0 a_{i0}}{\bar{U}_{eV}^{\frac{3}{2}}}\int_{\mathcal{E}_i}^{\infty}\frac{2}{3}\bar{U}_{eV}(\mathcal{U}-\mathcal{U}_i)\frac{2}{3}\bar{U}_{eV}\mathcal{U}\exp(-\mathcal{U})\frac{2}{3}\bar{U}_{eV}\,\mathrm{d}\mathcal{U} \ , \tag{XVII.3}$$

from which:

$$\langle \nu_i \rangle = \frac{8}{9}\sqrt{\frac{3e}{m_e\pi}}\,p_0 a_{i0}\,\bar{U}_{eV}^{\frac{3}{2}}\int_{\mathcal{U}_i}^{\infty}(\mathcal{U}-\mathcal{U}_i)\mathcal{U}\exp(-\mathcal{U})\,\mathrm{d}\mathcal{U} \ . \tag{3.303}$$

Equation (3.309) expressed as a function of the reduced energies $\mathcal{U}$ and $\mathcal{U}_i$

This equation reads:

$$\frac{2}{3}\bar{U}_{eV}\mu_i\left(\frac{2.405}{R}\right)^2 = 2\left(\frac{4}{3}\right)^{\frac{3}{2}}\sqrt{\frac{e}{m_e\pi}}\,a_{i0}p_0\,\bar{U}_{eV}^{\frac{3}{2}}\left(\frac{3}{4}\frac{\mathcal{E}_i}{\bar{U}_{eV}}\right)\exp\left(-\frac{3}{2}\frac{\mathcal{E}_i}{\bar{U}_{eV}}\right)\,. \tag{3.309}$$

Since $3\mathcal{E}_i/2\bar{U}_{eV} \equiv \mathcal{U}_i$, we can write:

$$\bar{U}_{eV}\mu_i\left(\frac{2.405}{R}\right)^2 = 2\sqrt{\frac{2e}{m_e\pi}}\,\frac{a_{i0}}{p_0}\,p_0^2\,\mathcal{E}_i^{\frac{1}{2}}\mathcal{U}_i^{\frac{1}{2}}\exp -\mathcal{U}_i \tag{XVII.4}$$

and then:

$$\mathcal{U}_i^{-\frac{1}{2}}\,(\exp\mathcal{U}_i) = \frac{2}{(2.405)^2}\sqrt{\frac{2e}{m_e\pi}}\underbrace{\left(\frac{a_{i0}\mathcal{E}_i^{\frac{1}{2}}}{\mu_i p_0}\right)}_{c_0^2}p_0^2R^2\,, \tag{XVII.5}$$

where $\mu_i p_0$ is the reduced ion mobility at 0°C, 1 torr (note the reference pressure here is 1 torr, rather than 760 torr).

Appendix XVIII
Propagation of an Electromagnetic Plane Wave in a Plasma and the Skin Depth

The propagation conditions of an electromagnetic (EM) wave in a plasma are governed by the four Maxwell equations, namely:

1. The Maxwell-Faraday equation:

$$\boldsymbol{\nabla} \wedge \boldsymbol{E} = -\frac{\partial \boldsymbol{B}}{\partial t} \ , \tag{2.2}$$

2. The Maxwell-Ampère equation:

$$\boldsymbol{\nabla} \wedge \boldsymbol{B} = \mu_0 \boldsymbol{J} + \mu_0 \epsilon_0 \frac{\partial \boldsymbol{E}}{\partial t} \ , \tag{2.3}$$

3. The Poisson (or Maxwell-Gauss) equation:

$$\boldsymbol{\nabla} \cdot \boldsymbol{E} = \frac{\rho}{\epsilon_0} \ , \tag{1.1}$$

4. The Maxwell-Thomson equation:

$$\boldsymbol{\nabla} \cdot \boldsymbol{B} = 0 \ . \tag{2.144}$$

Assuming that the plasma is neutral on the macroscopic scale ($\rho = 0$), and for the case of a dielectric description of the plasma (Sect. 2.2.1), (2.3) and (1.1) can be written, respectively:

$$\boldsymbol{\nabla} \cdot \boldsymbol{E} = 0 \tag{XVIII.1}$$

and:

$$\boldsymbol{\nabla} \wedge \boldsymbol{B} = \mu_0 \epsilon_0 \epsilon_p \frac{\partial \boldsymbol{E}}{\partial t} \ , \tag{2.45}$$

where ϵ_p represents the complex permittivity of the plasma relative to vacuum. The equation for the propagation of the EM wave is obtained by considering the rotational of (2.2):

$$\boldsymbol{\nabla} \wedge \boldsymbol{\nabla} \wedge \boldsymbol{E} = \boldsymbol{\nabla}(\boldsymbol{\nabla} \cdot \boldsymbol{E}) - \Delta \boldsymbol{E} = -\frac{\partial \boldsymbol{\nabla} \wedge \boldsymbol{B}}{\partial t} \ , \tag{XVIII.2}$$

M. Moisan, J. Pelletier, *Physics of Collisional Plasmas*,
DOI 10.1007/978-94-007-4558-2,

and then by taking account of (XVIII.1) and (2.45):

$$\Delta \boldsymbol{E} = \mu_0 \epsilon_0 \epsilon_p \frac{\partial^2 \boldsymbol{E}}{\partial t^2} \ . \tag{XVIII.3}$$

In the simple case of a plane EM wave (in the x, y plane) with angular frequency ω and propagating along the Oz axis, the electric field $\boldsymbol{E}$ can be written in the form:

$$\boldsymbol{E} = \boldsymbol{E}_0 \mathrm{e}^{\mathrm{i}(\omega t - k_z z)} \ , \tag{XVIII.4}$$

where k_z, the complex component along Oz of $\boldsymbol{k}$, the propagation vector (wavenumber[23]), can be written:

$$k_z = \beta + \mathrm{i}\alpha \ . \tag{XVIII.5}$$

Then from (XVIII.3) in Cartesian coordinates, we obtain the dispersion equation of a plane wave in an infinite homogeneous medium:

$$k_z^2 = \mu_0 \epsilon_0 \omega^2 \epsilon_p = \epsilon_p \left(\frac{\omega}{c}\right)^2 \ , \tag{XVIII.6}$$

where c is the speed of light in vacuum. In the general case, the permittivity ϵ_p of the plasma relative to vacuum can be written:

$$\epsilon_p = 1 + \frac{\sigma}{\mathrm{i}\omega\epsilon_0} \ , \tag{2.40}$$

or, taking account of the electric conductivity σ of electrons (2.39):

$$\epsilon_p = 1 - \frac{\omega_{pe}^2}{\omega(\omega - \mathrm{i}\nu)} \ . \tag{2.41}$$

From (XVIII.4) and (XVIII.5)), the electric field can be expressed as:

$$\boldsymbol{E} = \boldsymbol{E}_0 \mathrm{e}^{\mathrm{i}(\omega t - \beta z)} \mathrm{e}^{\alpha z} \ , \tag{XVIII.7}$$

which shows that the propagation of the wave is governed by β, the real part of k_z, while its attenuation is governed by α, the imaginary part of k_z. If k_z is strictly real ($\alpha = 0$), the wave propagates without any attenuation; if k_z includes a negative imaginary part ($\alpha < 0$), the wave is attenuated (a positive α value ($\alpha > 0$) would correspond to an amplification of the wave, which cannot be considered here as an acceptable physical solution). In the case of wave attenuation ($\alpha < 0$), the characteristic penetration depth δ_c of the HF field in the plasma is defined as the distance over which the field intensity of the plane EM wave reduces to 1/e (e is used exceptionally here for the base of the natural logarithm) of its initial value, i.e.:

$$\delta_c = \frac{1}{\Im(-k_z)} = -\frac{1}{\alpha} = \frac{(c/\omega)}{\Im\left(-\epsilon_p^{1/2}\right)} \ . \tag{XVIII.8}$$

The calculation of the skin depth can then be performed in a simple way for two particular cases:

Non-collisional plasmas: $\nu \ll \omega$

In this case ($\nu \ll \omega$), the value of the plasma permittivity (2.41), to a first approximation, is purely real:

$$\epsilon_p = 1 - \frac{\omega_{pe}^2}{\omega^2} \; . \tag{XVIII.9}$$

If the value of the permittivity is positive ($\omega_{pe} < \omega$), the wavenumber k_z is purely real ($k_z = \beta$) and the wave propagates without attenuation. If the value of the permittivity is negative ($\omega_{pe} > \omega$), the wavenumber k_z is totally imaginary ($k_z = \mathrm{i}\alpha$) and the wave cannot propagate in the plasma. In this latter case, the EM wave is reflected by the plasma (the plasma can be considered as a highly conductive medium) at the same time that there is attenuation of the HF field in the plasma along the z axis, related to the skin depth obtained from (XVIII.8):

$$\delta_c = \frac{c}{(\omega_{pe}^2 - \omega^2)^{1/2}} \simeq \frac{c}{\omega_{pe}} \; . \tag{XVIII.10}$$

Remark: The transition from the condition of propagation to that of no propagation of the EM plane wave (wave propagation cut-off) in a non-collisional plasma is obtained for the singular value $\epsilon_p = 0$ (or $k_z = 0$) resulting from the equality $\omega_{pe} = \omega$. The corresponding electron density n_c, the so-called *critical density* above which there is no propagation of a plane wave in a non-collisional plasma, is given by:

$$n_c = \frac{\epsilon_0 m_e \omega^2}{e^2} \; . \tag{XVIII.11}$$

Collisional plasmas: $\nu \gg \omega$

In this opposite case ($\nu \gg \omega$), the plasma permittivity of a high density plasma ($\omega_{pe} \gg \omega$) can be obtained from (2.41) as:

$$\epsilon_p = 1 - \frac{\mathrm{i}\omega_{pe}^2}{\nu\omega} \simeq -\frac{\mathrm{i}\omega_{pe}^2}{\nu\omega} \; . \tag{XVIII.12}$$

The complex square root of ϵ_p that corresponds to a physical solution for k_z can be written as:

$$\epsilon_p^{1/2} \simeq (1-\mathrm{i})\left(\frac{\omega_{pe}^2}{2\nu\omega}\right)^{1/2} . \tag{XVIII.13}$$

From (XVIII.8), the skin depth then takes the form:

$$\delta_c = \frac{c}{\omega_{pe}}\left(\frac{2\nu}{\omega}\right)^{1/2} , \tag{XVIII.14}$$

which, this time, depends on the collision frequency ν of the electrons and the angular frequency ω of the HF field. The wavenumber, derived from (XVIII.6) and (XVIII.14), can be expressed in the form:

$$k_z = \frac{1-\mathrm{i}}{\delta_c} ,$$

which implies that, in a high density collisional plasma (ω_{pe} and $\nu \gg \omega$), the EM wave can propagate over a distance equal to the skin depth even though $\omega_{pe} > \omega$.

Remark: The electric conductivity of electrons:

$$\sigma = \frac{n_e^2}{m_e(\nu + \mathrm{i}\omega)} \tag{2.39}$$

in a collisional plasma ($\nu \gg \omega$), takes the purely real value:

$$\sigma = \frac{n_e^2}{m_e\nu} . \tag{XVIII.15}$$

In this case, the skin depth (XVIII.14) can be written in the form:

$$\delta_c = \left(\frac{2}{\sigma\omega\mu_0}\right)^{1/2} , \tag{XVIII.16}$$

which is an expression that exactly corresponds to the well-known penetration depth formula of a plane wave in metallic conductors.

Appendix XIX
Surface-Wave Plasmas (SWP)

This class of HF plasma has played a determining role in the understanding and modelling of the plasmas generated by RF and microwave fields, and even for the positive column of DC discharges. This is due, on one hand, to the great flexibility of the operating conditions for SWP and, on the other hand, to their intrinsic properties. The following brief overview of SWP will aid the reader to better comprehend how some of the results presented in Chap. 4 have been obtained.

Figure XIX.1 shows schematically the way in which an SWP is generated in a cylindrical dielectric tube (planar or flat SWPs can also be created). Note that the HF field applicator, in this case a wave launcher, covers only a small length of the plasma column which is produced. This is because the discharge is sustained, at each point along the column, by the propagation of an electromagnetic (EM) wave, which is excited from the launching gap (typically a few mm wide) of the field applicator. The propagating medium of the wave consists of the plasma, the dielectric tube containing it, the air surrounding the tube and, in some cases, a hollow cylindrical conductor enclosing the whole system and coaxial to it. The EM wave is referred to as a surface wave, because the intensity of its field $\boldsymbol{E}$ is a maximum, radially, at the plasma-tube interface of the discharge, such that the wave seems to cling to the discharge tube and, in fact should the case arise, follows the variations in its diameter and curvature, if they are not too abrupt.

A surface wave is excited in both the forward and backward directions from the launching gap, as shown in Fig. XIX.1. With some types of launchers (for example, a surfaguide), the forward column is symmetric to the backward column, with respect to the gap, while in contrast, with some other launchers (for example, a surfatron), the plasma is almost exclusively that of the forward column. The power flow $P(z)$ emerging from the launching gap attenuates along the discharge vessel as the wave transfers its energy to the gas in the discharge that it creates.

One particular property of SWP is that the power lost by the wave $\mathrm{d}P(z)/\mathrm{d}z$ between z and $z + \mathrm{d}z$ is absorbed by the discharge over the same

M. Moisan, J. Pelletier, *Physics of Collisional Plasmas*,
DOI 10.1007/978-94-007-4558-2,

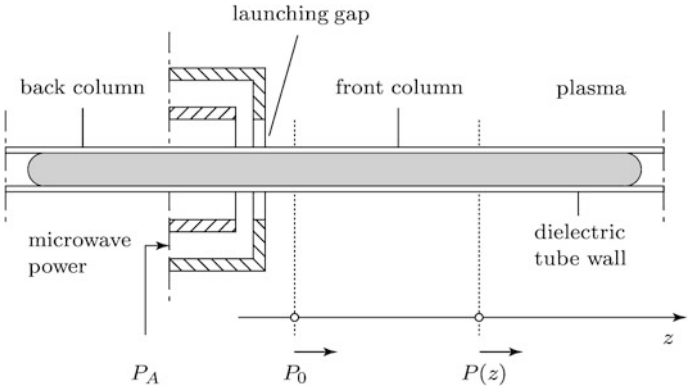

Fig. XIX.1 Schematic of the principle of formation of a plasma column generated by an electromagnetic surface wave in a dielectric tube, from the launching gap of a field applicator.

axial range z and $z + \mathrm{d}z$ (this is not true of HF plasmas in general), which simplifies the modelling.

The result of the progressive reduction in power flow $P(z)$ from the launching gap is a decrease, usually linear, in the electron density, as shown in Fig. XIX.2. In this figure, we further note that the slope of the curves becomes steeper as the wave frequency increases. In the low pressure case ($\nu/\omega \ll 1$), the wave ceases to propagate, and hence does not maintain a discharge, when n_e is below a certain value[189], while in the high pressure case, the wave ceases to propagate when the power flow is no longer sufficient to maintain the discharge, which determines, in both cases, the end of the plasma column.

Another remarkable property of SWPs, at least at pressures much below atmospheric pressure, is that an increase in the HF power delivered to the field applicator produces an increase in the length of the plasma column, without modifying the pre-existing segment of plasma with respect to the end of the column, this plasma segment being simply pushed away as a whole from the launching gap. Figure XIX.2 at 100 MHz is a good illustration of this behaviour of SWPs. The arrow indicating 36 W represents the axial position occupied by the applicator with respect to the end of the column ($z \simeq 0$) and we can see, as noted above, that the segment of the plasma column is not modified when the HF power is increased to 58 W. The average electron density $\bar{n}_e$ across a radial section of the plasma:

$$\overline{n_e}(z) = \frac{1}{\pi R^2} \int_0^R n_e(r, z)\, 2\pi r \mathrm{d}r \qquad \text{(XIX.1)}$$

[189] The minimum value of $\bar{n}_e$ in this case is $\bar{n}_e \simeq 1.2 \times 10^4 (1 + \epsilon_v) f^2$ (cm^{-3}) where $\epsilon_v$is the relative permittivity of the discharge tube (for example, 3.78 for fused silica) and f is the wave frequency, expressed in MHz.

of the additional segment is higher, but its gradient $\mathrm{d}\bar{n}_e/\mathrm{d}z$ remains the same. Note that, for a frequency of 27 MHz and a pressure of 30 mtorr (4 Pa), the plasma column in argon extends to 4.5 m with less than 40 W transmitted to the surfatron.

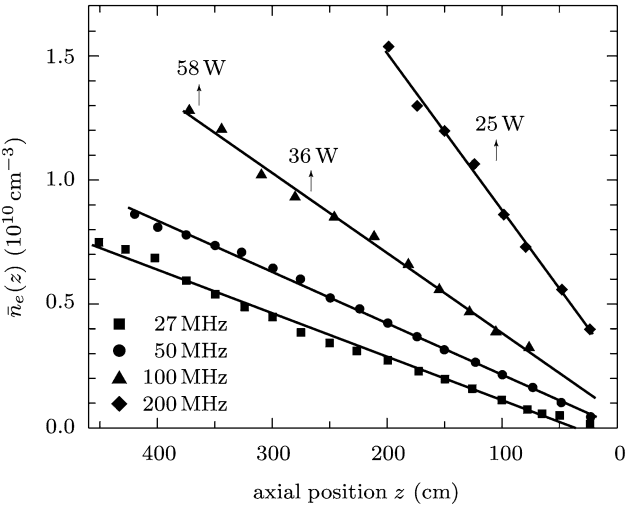

Fig. XIX.2 Axial distribution of the electron density observed along a plasma column, produced by a surface wave, at different excitation frequencies (tube radius $R = 6.4$ cm in free air, surfatron, argon 30 mtorr).

Figure XIX.3 shows that the value of $\bar{n}_e$ and its gradient $\mathrm{d}\bar{n}_e/\mathrm{d}z$ increase as the tube diameter is increased. This property is true for plasmas from atmospheric pressure (Fig. XIX.3) down to a few mtorr, and is related to the axial variation of the attenuation coefficient α of the surface wave [25]. This emphasises the fact that, given a plasma column along which $\bar{n}_e$ and $P(z)$ vary, we are able to perform a self-consistent study of the wave and plasma properties at each axial position z, without the need to modify the operating conditions. Having access to such a tremendous amount of data (from experiment and model) is another important and unique feature of SWP.

The range of possible operating conditions is the largest of all HF plasmas, and this makes it an instrument of choice for modelling, allowing ready comparison between experiment and theory, during which only one operating parameter can be modified at a time. As a matter of fact, it is possible to create these plasmas at frequencies from as low as 150 kHz to at least 2.45 GHz[190], producing a surface wave with the same azimuthal symmetry, i.e. the same EM configuration; we believe that this is not possible with any other

[190] SWPs have been achieved at 40 GHz. However, it is not clear whether the discharge was sustained on the $m = 0$ (azimuthally symmetric) surface wave mode [40].

type of HF discharges, since it would require changing the tube diameter or the type of field applicator, i.e. the EM field configuration, to cover such a large frequency domain. The range of pressures can extend from a few mtorr (much less even, in the presence of a confining magnetic field at ECR) up to at least 7 times atmospheric pressure, which we have been able to achieve, with the same EM field configuration. The diameter of the discharge tubes can range from less than 1 mm, up to 300 mm, for frequencies that are not too high (some restrictions apply, in effect, to the maximum discharge diameter, to avoid higher EM modes of the surface wave when the wave frequency is increased [18]. Due to this extreme adaptability of the operating conditions, we can say that the main application of SWPs is the modelling of HF plasmas, although there are now numerous industrial applications of SWPs.

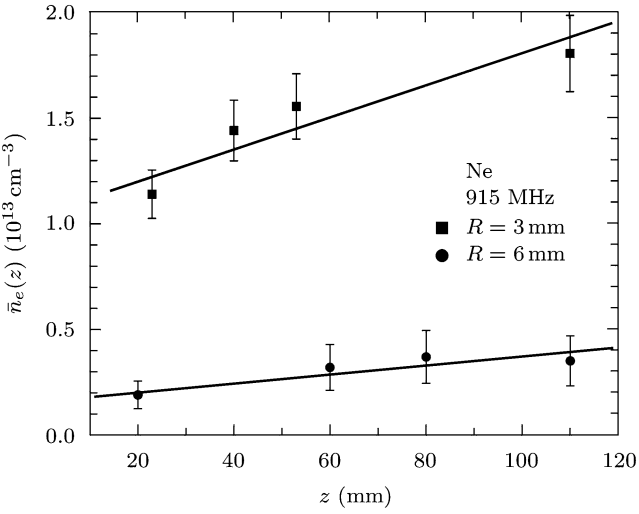

Fig. XIX.3 Axial distribution of the average electron density across a section of the discharge tube, for two values of internal radius (3 and 6 mm) in a neon plasma at 915 MHz, at atmospheric pressure.

Appendix XX
Useful Integrals and Expressions for the Differential Operators in Various Coordinate Systems

Useful integrals

Γ Function

$$\Gamma(x) = \int_0^\infty t^{z-1} \mathrm{e}^{-t}\, \mathrm{d}t\,, \quad \Re(z) > 0 \tag{XX.1}$$

For $z = n$, where n is an integer:

$$\Gamma(n) = (n-1)!\,, \quad \Gamma(n+1) = n\Gamma(n)\,.$$

Noteworthy values for the Γ function:

$$\Gamma\left(\frac{1}{2}\right) = \sqrt{\pi}\,, \quad \Gamma\left(\frac{3}{2}\right) = \frac{1}{2}\Gamma\left(\frac{1}{2}\right) = \frac{\sqrt{\pi}}{2}\,, \quad \Gamma(1) = 1\,.$$

Other integrals

$$\int_{-\infty}^{\infty} \mathrm{e}^{-y^2}\, \mathrm{d}y = \sqrt{\pi} \tag{XX.2}$$

$$E(n) = \int_{-\infty}^{\infty} \mathrm{e}^{-ax^2} x^n\, \mathrm{d}x \qquad a > 0\,, \tag{XX.3}$$

$$E(n) = 0 \qquad \text{for } n \text{ odd},$$

$$E(n) = 2\int_0^\infty \mathrm{e}^{-ax^2} x^n\, \mathrm{d}x = \frac{\Gamma\left(\frac{n+1}{2}\right)}{a^{\left(\frac{n+1}{2}\right)}} \qquad \text{for } n \text{ even}.$$

M. Moisan, J. Pelletier, *Physics of Collisional Plasmas*,
DOI 10.1007/978-94-007-4558-2,

Noteworthy values

$$E(n) = \frac{1}{2}\Gamma\left(\frac{n+1}{2}\right) a^{-\frac{n+1}{2}} ,$$

$$E(0) = \frac{1}{2}\Gamma\left(\frac{1}{2}\right) a^{-\frac{1}{2}} = \frac{\sqrt{\pi}}{2} a^{-\frac{1}{2}} , \qquad E(1) = \frac{1}{2}\Gamma(1)\, a^{-1} = \frac{1}{2} a^{-1} ,$$

$$E(2) = \frac{1}{2}\Gamma\left(\frac{3}{2}\right) a^{-\frac{3}{2}} = \frac{\sqrt{\pi}}{4} a^{-\frac{3}{2}} , \qquad E(3) = \frac{1}{2}\Gamma(2)\, a^{-2} = \frac{1}{2} a^{-2},$$

$$E(4) = \frac{1}{2}\Gamma\left(\frac{5}{2}\right) a^{-\frac{5}{2}} = \frac{3\sqrt{\pi}}{8} a^{-\frac{5}{2}} , \qquad E(5) = \frac{1}{2}\Gamma(3)\, a^{-3} = a^{-3} .$$

Expression for the differential operators in an arbitrary coordinate system (orthogonal, rectilinear and curvilinear coordinates)

If x^1, x^2 and x^3 are the system coordinates and e_1, e_2, and e_3 are the (local) scale factors, we can express the differential operators in the following manner:

- The gradient

$$\boldsymbol{\nabla} = \left(\frac{1}{e_1}\partial_1,\ \frac{1}{e_2}\partial_2,\ \frac{1}{e_3}\partial_3\right) , \tag{XX.4}$$

  where $\partial_i \equiv \partial/\partial x^i$.

- The curl of a vector

$$\boldsymbol{\nabla} \wedge \boldsymbol{A} = \left(\frac{1}{e_2 e_3}(\partial_2 e_3 A_3 - \partial_3 e_2 A_2),\ \frac{1}{e_3 e_1}(\partial_3 e_1 A_1 - \partial_1 e_3 A_3),\right.$$
$$\left.\frac{1}{e_1 e_2}(\partial_1 e_2 A_2 - \partial_2 e_1 A_1)\right) . \tag{XX.5}$$

- The divergence of a vector

$$\boldsymbol{\nabla} \cdot \boldsymbol{A} = \frac{1}{e_1 e_2 e_3}(\partial_1 e_2 e_3 A_1 + \partial_2 e_3 e_1 A_2 + \partial_3 e_1 e_2 A_3) . \tag{XX.6}$$

- The Laplacian of a scalar

$$\Delta\phi = \frac{1}{e_1 e_2 e_3}\left(\partial_1 \frac{e_2 e_3}{e_1}\partial_1\phi + \partial_2 \frac{e_3 e_1}{e_2}\partial_2\phi + \partial_3 \frac{e_1 e_2}{e_3}\partial_3\phi\right) . \tag{XX.7}$$

- The Laplacian of a vector in Cartesian coordinates

$$\Delta \boldsymbol{A} = \Delta A_1 \hat{\mathbf{e}}_1 + \Delta A_2 \hat{\mathbf{e}}_2 + \Delta A_3 \hat{\mathbf{e}}_3 \,. \tag{XX.8}$$

Quite generally:

$$\Delta \boldsymbol{A} = \boldsymbol{\nabla}(\boldsymbol{\nabla} \cdot \boldsymbol{A}) - \boldsymbol{\nabla} \wedge \boldsymbol{\nabla} \wedge \boldsymbol{A} \,. \tag{XX.9}$$

These operators have the following properties:

- The curl of a gradient is zero

$$(\boldsymbol{\nabla} \wedge \boldsymbol{\nabla}\phi)_1 = \frac{1}{e_2 e_3}\left(\partial_2 e_3 \frac{1}{e_3}\partial_3\phi - \partial_3 e_2 \frac{1}{e_2}\partial_2\phi\right) = \frac{1}{e_2 e_3}(\partial_2\partial_3 - \partial_3\partial_2) = 0 \,, \tag{XX.10}$$

and similarly for the two other components.

- The divergence of the curl of a vector is zero

$$(\boldsymbol{\nabla} \cdot \boldsymbol{\nabla} \wedge \boldsymbol{A}) = \frac{1}{e_1 e_2 e_3}\Bigg(\partial_1 e_2 e_2 \frac{1}{e_2 e_3}(\partial_2 e_3 A_3 - \partial_3 e_2 A_2) + \partial_2 e_3 e_1 \frac{1}{e_3 e_1}(\partial_3 e_1 A_1 - \partial_1 e_3 A_3) + \partial_3 e_1 e_2 \frac{1}{e_1 e_2}(\partial_1 e_2 A_2 - \partial_2 e_1 A_1)\Bigg) = 0 \,. \tag{XX.11}$$

- The divergence of the gradient of a scalar is equal to the Laplacian

$$\boldsymbol{\nabla} \cdot \boldsymbol{\nabla}\phi = \frac{1}{e_1 e_2 e_3}\left(\partial_1 \frac{e_2 e_3}{e_1}\partial_1\phi + \partial_2 \frac{e_3 e_1}{e_2}\partial_2\phi + \partial_3 \frac{e_1 e_2}{e_3}\partial_3\right)\phi = \Delta\phi \,. \tag{XX.12}$$

Curvilinear, orthogonal, coordinate systems and scale factors

Cartesian coordinates

The variables are $x^1 = x$, $x^2 = y$ and $x^3 = z$ and the scale factors are $e_1 = e_2 = e_3 = 1$.

$$\boldsymbol{\nabla}\phi = \frac{\partial\phi}{\partial x}\hat{\mathbf{e}}_x + \frac{\partial\phi}{\partial y}\hat{\mathbf{e}}_y + \frac{\partial\phi}{\partial z}\hat{\mathbf{e}}_z \tag{XX.13}$$

$$\boldsymbol{\nabla} \cdot \boldsymbol{A} = \frac{\partial A_x}{\partial x} + \frac{\partial A_y}{\partial y} + \frac{\partial A_z}{\partial z} \tag{XX.14}$$

$$\boldsymbol{\nabla} \wedge \boldsymbol{A} = \left(\frac{\partial A_z}{\partial y} - \frac{\partial A_y}{\partial z}\right)\hat{\mathbf{e}}_x + \left(\frac{\partial A_x}{\partial z} - \frac{\partial A_z}{\partial x}\right)\hat{\mathbf{e}}_y + \left(\frac{\partial A_y}{\partial x} - \frac{\partial A_x}{\partial y}\right)\hat{\mathbf{e}}_z \tag{XX.15}$$

$$\Delta\phi = \frac{\partial^2\phi}{\partial x^2} + \frac{\partial^2\phi}{\partial y^2} + \frac{\partial^2\phi}{\partial z^2} \tag{XX.16}$$

$$\begin{aligned}\Delta\boldsymbol{A} = &\left(\frac{\partial^2 A_x}{\partial x^2} + \frac{\partial^2 A_x}{\partial y^2} + \frac{\partial^2 A_x}{\partial z^2}\right)\hat{\mathbf{e}}_x + \left(\frac{\partial^2 A_y}{\partial x^2} + \frac{\partial^2 A_y}{\partial y^2} + \frac{\partial^2 A_y}{\partial z^2}\right)\hat{\mathbf{e}}_y \\ &+ \left(\frac{\partial^2 A_z}{\partial x^2} + \frac{\partial^2 A_z}{\partial y^2} + \frac{\partial^2 A_z}{\partial z^2}\right)\hat{\mathbf{e}}_z\end{aligned} \tag{XX.17}$$

$$\begin{aligned}(\boldsymbol{A}\cdot\boldsymbol{\nabla})\boldsymbol{B} = &\left(A_x\frac{\partial B_x}{\partial x} + A_y\frac{\partial B_x}{\partial y} + A_z\frac{\partial B_x}{\partial z}\right)\hat{\mathbf{e}}_x \\ &+ \left(A_x\frac{\partial B_y}{\partial x} + A_y\frac{\partial B_y}{\partial y} + A_z\frac{\partial B_y}{\partial z}\right)\hat{\mathbf{e}}_y \\ &+ \left(A_x\frac{\partial B_z}{\partial x} + A_y\frac{\partial B_z}{\partial y} + A_z\frac{\partial B_z}{\partial z}\right)\hat{\mathbf{e}}_z\end{aligned} \tag{XX.18}$$

Cylindrical coordinates

The variables are $x^1 = r$, $x^2 = \theta$ and $x^3 = z$ and the scale factors are $e_1 = 1$, $e_2 = r$, $e_3 = 1$.

$$\boldsymbol{\nabla}\phi = \frac{\partial\phi}{\partial r}\hat{\mathbf{e}}_r + \frac{1}{r}\frac{\partial\phi}{\partial\theta}\hat{\mathbf{e}}_\theta + \frac{\partial\phi}{\partial z}\hat{\mathbf{e}}_z \tag{XX.19}$$

$$\boldsymbol{\nabla}\cdot\boldsymbol{A} = \frac{1}{r}\frac{\partial(rA_r)}{\partial r} + \frac{1}{r}\frac{\partial A_\theta}{\partial\theta} + \frac{\partial A_z}{\partial z} \tag{XX.20}$$

$$\begin{aligned}\boldsymbol{\nabla}\wedge\boldsymbol{A} = &\left(\frac{1}{r}\frac{\partial A_z}{\partial\theta} - \frac{\partial A_\theta}{\partial z}\right)\hat{\mathbf{e}}_r + \left(\frac{\partial A_r}{\partial z} - \frac{\partial A_z}{\partial r}\right)\hat{\mathbf{e}}_\theta \\ &+ \frac{1}{r}\left(\frac{\partial(rA_\theta)}{\partial r} - \frac{\partial A_r}{\partial\theta}\right)\hat{\mathbf{e}}_z\end{aligned} \tag{XX.21}$$

$$\Delta\phi = \frac{1}{r}\frac{\partial}{\partial r}\left(r\frac{\partial\phi}{\partial r}\right) + \frac{1}{r^2}\frac{\partial^2\phi}{\partial\theta^2} + \frac{\partial^2\phi}{\partial z^2} \tag{XX.22}$$

$$\begin{aligned}\Delta\boldsymbol{A} = &\left(\Delta A_r - \frac{2}{r^2}\frac{\partial A_\theta}{\partial\theta} - \frac{A_r}{r^2}\right)\hat{\mathbf{e}}_r \\ &+ \left(\Delta A_\theta - \frac{2}{r^2}\frac{\partial A_r}{\partial\theta} - \frac{A_\theta}{r^2}\right)\hat{\mathbf{e}}_\theta + \Delta A_z\hat{\mathbf{e}}_z\end{aligned} \tag{XX.23}$$

$$(\boldsymbol{A}\cdot\boldsymbol{\nabla})\boldsymbol{B} = \left(A_r\frac{\partial B_r}{\partial r} + \frac{A_\theta}{r}\frac{\partial B_r}{\partial \theta} + A_z\frac{\partial B_r}{\partial z} - \frac{A_\theta B_\theta}{r}\right)\hat{\mathbf{e}}_r + \left(A_r\frac{\partial B_\theta}{\partial r} + \frac{A_\theta}{r}\frac{\partial B_\theta}{\partial \theta} + A_z\frac{\partial B_\theta}{\partial z} + \frac{A_\theta B_r}{r}\right)\hat{\mathbf{e}}_\theta + \left(A_r\frac{\partial B_z}{\partial r} + \frac{A_\theta}{r}\frac{\partial B_z}{\partial \theta} + A_z\frac{\partial B_z}{\partial z} +\right)\hat{\mathbf{e}}_z \tag{XX.24}$$

Spherical coordinates

The variables are $x^1 = r$, $x^2 = \theta$ and $x^3 = \varphi$ and scale factors are $e_1 = 1$, $e_2 = r$, $e_3 = r\sin\theta$.

$$\boldsymbol{\nabla}\phi = \frac{\partial\phi}{\partial r}\hat{\mathbf{e}}_r + \frac{1}{r}\frac{\partial\phi}{\partial\theta}\hat{\mathbf{e}}_\theta + \frac{1}{r\sin\theta}\frac{\partial\phi}{\partial\varphi}\hat{\mathbf{e}}_\varphi \tag{XX.25}$$

$$\boldsymbol{\nabla}\cdot\boldsymbol{A} = \frac{1}{r^2}\frac{\partial(r^2A_r)}{\partial r} + \frac{1}{r\sin\theta}\frac{\partial(A_\theta\sin\theta)}{\partial\theta} + \frac{1}{r\sin\theta}\frac{\partial A_\varphi}{\partial\varphi} \tag{XX.26}$$

$$\boldsymbol{\nabla}\wedge\boldsymbol{A} = \frac{1}{r\sin\theta}\left(\frac{\partial(A_\varphi\sin\theta)}{\partial\theta} - \frac{\partial A_\theta}{\partial\varphi}\right)\hat{\mathbf{e}}_r + \frac{1}{r}\left(\frac{1}{\sin\theta}\frac{\partial A_r}{\partial\varphi} - \frac{\partial(rA_\varphi)}{\partial r}\right)\hat{\mathbf{e}}_\theta + \frac{1}{r}\left(\frac{\partial(rA_\theta)}{\partial r} - \frac{\partial A_r}{\partial\theta}\right)\hat{\mathbf{e}}_\varphi \tag{XX.27}$$

$$\Delta\phi = \frac{1}{r^2}\frac{\partial}{\partial r}\left(r^2\frac{\partial\phi}{\partial r}\right) + \frac{1}{r^2\sin\theta}\frac{\partial}{\partial\theta}\left(\sin\theta\frac{\partial\phi}{\partial\theta}\right) + \frac{1}{r^2\sin^2\theta}\frac{\partial^2\phi}{\partial\varphi^2} \tag{XX.28}$$

$$\Delta\boldsymbol{A} = \left(\Delta A_r - \frac{2A_r}{r^2} - \frac{2}{r^2}\frac{\partial A_\theta}{\partial\theta} - \frac{2A_\theta\cot\theta}{r^2} - \frac{2}{r^2\sin\theta}\frac{\partial A_\varphi}{\partial\varphi}\right)\hat{\mathbf{e}}_r + \left(\Delta A_\theta + \frac{2}{r^2}\frac{\partial A_r}{\partial\theta} - \frac{A_\theta}{r^2\sin^2\theta} - \frac{2\cos\theta}{r^2\sin^2\theta}\frac{\partial A_\varphi}{\partial\varphi}\right)\hat{\mathbf{e}}_\theta + \left(\Delta A_\varphi - \frac{A_\varphi}{r^2\sin^2\theta} + \frac{2}{r^2\sin\theta}\frac{\partial A_r}{\partial\varphi} + \frac{2\cos\theta}{r^2\sin^2\theta}\frac{\partial A_\theta}{\partial\varphi}\right)\hat{\mathbf{e}}_\varphi \tag{XX.29}$$

$$
\begin{aligned}
(\boldsymbol{A}\cdot\boldsymbol{\nabla})\boldsymbol{B} = &\left(A_r\frac{\partial B_r}{\partial r}+\frac{A_\theta}{r}\frac{\partial B_r}{\partial\theta}+\frac{A_\varphi}{r\sin\theta}\frac{\partial B_r}{\partial\varphi}-\frac{A_\theta B_\theta+A_\varphi B_\varphi}{r}\right)\hat{\mathbf{e}}_r\\
&+\left(A_r\frac{\partial B_\theta}{\partial r}+\frac{A_\theta}{r}\frac{\partial B_\theta}{\partial\theta}+\frac{A_\varphi}{r\sin\theta}\frac{\partial B_\theta}{\partial\varphi}+\frac{A_\theta B_r}{r}-\frac{A_\varphi B_\varphi\cot\theta}{r}\right)\hat{\mathbf{e}}_\theta\\
&+\left(A_r\frac{\partial B_\varphi}{\partial r}+\frac{A_\theta}{r}\frac{\partial B_\varphi}{\partial\theta}+\frac{A_\varphi}{r\sin\theta}\frac{\partial B_\varphi}{\partial\varphi}+\frac{A_\varphi B_r}{r}+\frac{A_\varphi B_\theta\cot\theta}{r}\right)\hat{\mathbf{e}}_\varphi
\end{aligned}
\tag{XX.30}
$$

References

[1] Allis, W.P., Rose, D.J., *Phys. Rev.* **93**, 84 (1954)
[2] Allis, W.P., *Handbuch der Physik* **21**, 383 (1956) (Springer Verlag, Berlin)
[3] Calzada, M.D., Moisan, M., Gamero, A., Sola, A., *J. Appl. Phys.* **80**, 46 (1996)
[4] Castaños Martìnez, E., Kabouzi, Y., Makasheva, K., Moisan, M., *Phys. Rev. E* **70**, 066405 (2004)
[5] Castaños Martìnez, E., Moisan, M., *52nd Annual Technical Conference Proceedings of the Society of Vacuum Coaters*, 333 (2009)
[6] Castaños Martìnez, E., Moisan, M., Kabouzi, Y., *J. Phys. D: Appl. Phys.* **42**, 012003 (2009)
[7] Castaños Martìnez, E., Moisan, M., *IEEE Trans. Plasma Sci.* **39**, 2192 (2011)
[8] Claude, R., Moisan, M., Wertheimer, M.R., Zakrzewski, Z., *Plasma Chem. Plasma Proc.* **7**, 451 (1987)
[9] Cramer, W.H., Simons, J.H., *J. Chem. Phys.* **26**, 1272 (1957)
[10] Druyvesteyn, M.J., Penning, F.M., *Rev. Mod. Phys.* **12**, 87 (1940)
[11] Ferreira, C.M., Loureiro, J., *J. Phys. D: Appl. Phys.* **16**, 2471 (1983)
[12] Fozza, A.C., Moisan, M., Wertheimer, M.R., *J. Appl. Phys.* **88**, 20 (2000)
[13] Golubovskii, Yu.B., Sonneburg, R., *Zh. Tekh. Fiz.* **49**, 295 (1979) [*Sov. Phys.Tech. Phys.* **24**, 179 (1979)]
[14] Hansen, C., Reimann, A.B., Fajans, J., *Phys. Plasmas* **3**, 1820 (1996)
[15] Kabouzi, Y., Calzada, M.D., Moisan, M., Tran, K.C., Trassy, C., *J. Appl. Phys.* **91**, 1008 (2002)
[16] Koleva, I., Makasheva, K., Paunska, Ts., Schlueter, H., Shivarova, A., Tarnev, Kh., *Contrib. Plasma Phys.* **44** 552 (2004)
[17] Makasheva, K., Shivarova, A., *Phys. Plasmas* **8**, 836 (2001)
[18] Margot-Chaker, J., Moisan, M., Chaker, M., Glaude, V.M.M., Lauque, P., Paraszczak, J. and Sauvé, G., *J. Appl. Phys.* **66** 4134 (1989)
[19] Margot, J., Moisan, M., *J. Phys. D: Appl. Phys.* **24**, 1765 (1991)
[20] Margot, J., Moisan, M., chapter 8 of [26]
[21] McDaniel, E.W., *Collision phenomena in ionized gases* (Wiley, 1964)

M. Moisan, J. Pelletier, *Physics of Collisional Plasmas*,
DOI 10.1007/978-94-007-4558-2,

[22] Microwave discharges: fundamentals and applications, edited by C.M. Ferreira, M. Moisan, *NATO ASI series B: Physics* **302** (Plenum, New York, 1993)
[23] Moisan, M., Zakrzewski, Z., in *Radiative Processes in Discharge Plasmas*, edited by J.M. Proud, L.H. Luessen (Plenum, New York, 1986) p. 381
[24] Moisan, M., Barbeau, C., Claude, R., Ferreira, C.M., Margot, J., Paraszczak, J., Sá, A.B., Sauvé, G., Wertheimer, M.R., *J. Vac. Sci. Technol.* **B9**, 8 (1991)
[25] Moisan, M., Zakrzewski, Z., *J. Phys. D: Appl. Phys.* **24**, 1025 (1991)
[26] Moisan, M., Pelletier, J., *Microwave excited plasmas* (Elsevier, Amsterdam, 1992)
[27] Nachtrieb, R., Khan, F., Waymouth, J.F., *J. Phys. D: Appl. Phys.* **38**, 3226–3236 (2005)
[28] Nickel, J.C., Parker, J.V., Gould, R.W., *Phys. Rev. Lett.* **11**, 183 (1963)
[29] Royal, J., Orel, A.E., *Phys. Rev. A* **73**, 042706 (2006)
[30] Pollak, J., Moisan, M., Zakrzewski, Z., *Plasma Sources Sci. Technol.* **16**, 310 (2007)
[31] Ramsauer, C., Kollath, R., *Ann. Phys.* **12**, 527 (1932)
[32] Rose, D.J., Brown, S.C., *Phys. Rev.* **98**, 310 (1955)
[33] Sá, P.A., Loureiro, J., Ferreira, C.M., *J. Phys. D: Appl. Phys.* **25**, 960 (1992). Also see C.M. Ferreira, M. Moisan, chapter 3 of [26]
[34] Sá, P.A., Loureiro, J., Ferreira, C.M., *J. Phys. D: Appl. Phys.* **27**, 1171 (1994)
[35] Sauvé, G., Moisan, M., Paraszczak, J., Heidenreich, J., *Appl. Phys. Lett.* **53**, 470 (1988)
[36] Schlüter, H., Shivarova, A., *Physics Reports* **443**, 121 (2007)
[37] Simons, J.H., Fontana, C.M., Muschlitz Jr., E.E., Jackson, S.R., *J. Chem. Phys.* **11**, 307 (1943)
[38] Simons, J.H., Fontana, C.M., Francis, H.T., Unger, L.G., *J. Chem. Phys.* **11**, 312 (1943)
[39] Simon, A., *Phys. Rev.* **98**, 317 (1955)
[40] Vikharev, A.L., Ivanov, O.A., Kolysko, A.L., *Technical Physics Letters*, **22**, 832 (1996)
[41] Winkler, R., Deutsch, H., Wilhelm, J., Wilke, Ch., *Beitr. Plasmaphys.* **24**, 285 (1984)
[42] Winkler, R., Wilhelm, J., Hess, A., *Annalen der Physik* **42**, 537 (1985)
[43] Zakrzewski, Z., Moisan, M., Sauvé, G., chapter 4 of [26]

Recommended Reading

General treatises on plasma physics

- Badareu, E., Popescu, E., *Gaz ionisés* (Dunod, 1965)
- Delcroix, J.L., *Introduction à la théorie des gaz ionisés* (Dunod, 1959)
- Delcroix, J.L., *Physique des plasmas*, T. I et II (Monographie Dunod, 1966)
- Delcroix, J.L., Bers, A., *Physique des plasmas*, T. 1 et T. 2 (Interéditions-CNRS, 1994)
- Held, B., *Physique des plasmas froids* (Masson, 1994)
- Moisan, M., Pelletier, J., *Physique des plasmas collisionnels* (EDP Sciences, 2006)
- Papoular, R., *Phénomènes électriques dans les gaz* (Dunod, 1963)
- Quémada, D., *Gaz et plasmas*, chapters 4 and 5 in *Traité d'électricité : l'électricité et la matière*, tome III, edited by G. Goudet (Masson, 1975)
- Rax, J.M., *Physique des plasmas* (Dunod, 2005)

- Chen, F.F., *Introduction to plasma physics and controlled fusion*, volume 1 (Plenum, 1984)
- Golant, V.E., Zhilinsky, A.P., Sakharov, I.E., *Fundamentals of plasma physics*, edited by S.C. Brown (Wiley, 1977)
- Gurnett, D.A., Bhattacharjee, A., *Introduction to plasma physics* (Cambridge University Press, 2005)
- Jancel, R., Kahan, Th., *Electrodynamics of Plasmas* (John Wiley and Sons, 1966)
- Lieberman, M.A., Lichtenberg, A.J., *Principles of plasma discharges and materials processing*, Second Edition (Wiley, 2005)
- Nishikawa, K., Wakatani, M., *Plasma physics* (Springer, 2000)
- Raizer, Yu.P., *Gas discharge physics* (Springer, 1997)
- Seshadri, S.R., *Fundamentals of plasma physics* (Elsevier, 1973)
- von Engel, A., *Ionized gases* (Clarendon Press, 1957)
- von Engel, A., *Electric plasmas: Their nature and uses* (Taylor and Francis, 1983)

M. Moisan, J. Pelletier, *Physics of Collisional Plasmas*,
DOI 10.1007/978-94-007-4558-2,

Treatises on specific topics of plasma physics

- Aliev, Yu.M., Schlüter, H., Shivarova, A., *Guided-wave-produced plasmas* (Springer, 2000)
- Chabert, P., Braithwaite, N., *Physics of Radio-Frequency Plasmas* (Cambridge University Press, 2011)
- Ferreira, C.M., Moisan, M., *Microwave Discharges* (Plenum Press, 1993)
- Geller, R., *Electron Cyclotron Resonance Ion Sources and ECR Plasmas* (IOP Publishing, 1996)
- Kando, M., Nagatsu, M. (eds.) *Proc. of the VIIth Int. Workshop on Microwave discharges: fundamentals and applications* (Shizuoka University, 2009)
- Lebedev, Yu.A. (ed.), *Proc. of the VIth Int. Workshop on Microwave discharges: fundamentals and applications* (Yanus-K, 2006)
- Moisan, M., Pelletier, J., *Microwave excited plasmas* (Elsevier, 1992)
- Popov, O.A., *High Density Plasma Sources* (Noyes Publications, 1995)
- Raizer, Yu.P., Shneider, M.N., Yatsenko, N.A., *Radio-frequency capacitive discharges* (CRC Press, 1995)
- Schlüter, H., Shivrova, A., *Advanced technologies Based on Wave and Beam Generated Plasmas* (Kluwer Academic Publishers, 1999)

- Artsimovitch, L., Loukianov, S., *Mouvement des particules chargées dans des champs électriques et magnétiques* (Ed. de Moscou, 1975)
- Brown, S.C., *Basic data of plasma physics* (MIT, 1959)
- Makabe, T. (ed.), *Advances in low temperature RF plasmas* (North-Holland, 2002)
- Massey, H.S., Burhop, E.H.S., *Electronic and ionic impact phenomena* (Oxford, 1952)
- McDaniel, E.W., *Collision phenomena in ionized gases* (Wiley, 1964)

- Allis, W.P., Buchsbaum, S.J., Bers, A., *Waves in anisotropic plasmas* (MIT, 1963)
- Quémada, D., *Ondes dans les plasmas* (Hermann, 1968)
- Vandenplas, P.E., *Electron waves and resonances in bounded plasmas* (Wiley, 1968)

- Auciello, O., Flamm, D.L. (eds.), *Plasma diagnostics* (Academic Press, 1989)
- Heald, M.A., Wharton, C.B., *Plasma diagnostics with microwaves* (Wiley, 1965)
- Ricard, A., *Reactive plasmas* (Société Française du Vide, 1996)

- Yvon, J., *Les corrélations et l'entropie* (Monographie Dunod, 1966)

- Collection du Commissariat à l'énergie atomique (CEA, France) publiée sous la direction de R. Dautray, *La fusion thermonucléaire contrôlée par confinement magnétique* (Masson, 1987)

Popular treatise on plasmas

- Bradu, P., *L'univers des plasmas* (Flammarion, 2002)

Further related reading

- Brillouin, L., *Les tenseurs en mécanique et en élasticité* (Masson, 1960)
- Landau, L., Lifchitz, E., *Mécanique des fluides* (Mir, 1989)
- Lorrain, P., Corson, D.P., Lorrain, F., *Electromagnetic fields and waves* (Freeman, 1987)

Index

M. Moisan, J. Pelletier, *Physics of Collisional Plasmas*,
DOI 10.1007/978-94-007-4558-2,